Supporting Information
for

In vitro anticancer activity and in vivo biodistribution of rhenium(I) tricarbonyl aqua complexes

Kevin M. Knopf,[†] Brendan L. Murphy,[†] Samantha N. MacMillan,[†] Jeremy M. Baskin,[†‡] Martin P. Barr,[§] Eszter Boros,[∥#] and Justin J. Wilson*[†]

[†]Department of Chemistry & Chemical Biology, Cornell University, Ithaca, NY 14853, USA. E-mail: jjw275@cornell.edu
[‡]Weill Institute for Cell & Molecular Biology, Cornell University, Ithaca, NY 14853, USA
[§]Thoracic Oncology Research Group, Trinity Translational Medicine Institute, Trinity Centre for Health Sciences, St. James's Hospital and Trinity College Dublin, Dublin, Ireland
[∥]A. A. Martinos Center for Biomedical Imaging, Massachusetts General Hospital, Harvard Medical School, 149 13th Street, Suite 2301, Charlestown, MA 02129, USA
#Present Address: Department of Chemistry, Stony Brook University, Stony Brook, NY 11790-3400, USA

Content	Table/Figure	Page
Experimental	-	S2
Infrared Spectra	Figure S1	S8
NMR Spectra	Figures S2–S8	S9
ESI-MS	Figures S9–S15	S12
Cell Viability Curves	Figures S16–S21	S16
Fluorescence Microscope Images	Figures S22–S24	S19
Cell Cycle Analysis	Figures S25–S26	S21
Annexin V/PI Assay Plots	Figure S27	S22
ROS Graph and Histograms	Figures S28–S29	S22
JC-1 Graph and Histograms	Figures S30–S31	S23
Cell Viability Curves with Inhibitors	Figures S32–S33	S24
Western Blots	Figure S34	S25
Uptake Histograms and Microscope Images	Figures S35–S38	S26
NCI-60 Single-Dose Mean Graph for 10 μM **13**	Figure S39	S28
Synthesis of **13***	Figure S40	S29
HPLC traces of **13** and **13***	Figure S41	S29
Biodistribution Table for **13** and **13***	Table S1	S30
Reagent Suppliers	Table S2	S31
Crystal Data and Structure Refinement Tables	Tables S3-S6	S32
References	-	S36

Experimental

Physical Measurements. ^{1}H NMR spectra were obtained on a Mercury 300 MHz NMR spectrometer and ^{19}F{^{1}H} NMR spectra were obtained on an INOVA 400 MHz NMR spectrometer. IR spectra were acquired with a Thermo Nicolet Avatar 370 DTGS FT-IR spectrometer and with samples prepared as KBr pellets. Elemental analyses (CHN) were performed by Atlantic Microlab Inc., Norcross, GA, USA. High-resolution mass spectra (HRMS) were recorded on an Exactive Orbitrap mass spectrometer in positive ESI mode (ThermoFisher Scientific, Waltham, MA).

Analytical high-performance liquid chromatography (HPLC) for rhenium complex analysis and capacity factor calculation was carried out with a Shimadzu LC20–AT HPLC and an SPD-20AV UV/Vis detector monitoring at 220 and 260 nm using the following method: Ultra Aqueous C18 column, 100 Å, 5 μm, 250 mm x 4.6 mm (Restek, Bellefonte, PA), 1 mL/min, mobile phase A: 0.1% TFA in water, mobile phase B: 0.1% TFA in MeOH; 0-5 min: 10% B, 5-25 min: 10-100% B.

For HPLC-ICP-MS, an Agilent 8800 ICP-MS (standard operating conditions with 40% O_2 cell gas in addition to 20% option gas (20% O_2, 80% Ar) when conducting reverse phase analysis) was used, interfaced with an Agilent 1260 series HPLC system from Agilent Technologies. HPLC method 2: C18 column (Phenomenex Gemini C18, 150 mm x 4.60 mm), 0.8 mL/min, mobile phase A (water, 0.1% TFA), mobile phase B (MeOH, 0.1% TFA), gradient: 0-2 min: 5% B; 2-14 min: 5-95% B; 14-16 min: 95% B; 16-16.5 min: 95-5% B; 16.5-20 min 5% B.

Analytical radio-HPLC was performed on an Agilent 1100 system 1 mL/min, and equipped with a radiation detector channel using the following method 3: C18 column (Phenomenex Luna C18(2), 100 mm x 2 mm), 1 mL/min, mobile phase A (water, 0.1% TFA), mobile phase B (MeOH, 0.1% TFA); 0-2 min: 5% B; 2-14 min: 5-95% B; 14-16 min.

Materials and Methods. All reagents were purchased from commercial vendors, as given in Table S2. The *fac*-[Re(CO)$_3$(NN)Cl] complexes (**1**–**7**) were synthesized according to a literature method.[1]

***fac*-[Re(CO)$_3$(NN)(H$_2$O)][OTf] (8–14)**. The complexes were synthesized according to a literature method.[2] In a typical procedure, *fac*-[Re(CO)$_3$(NN)Cl] (**1**–**7**) (0.11 mmol) and silver triflate (28 mg, 0.11 mmol) were combined in 3 mL acetone and heated to reflux for 2 h in the dark. The solution was filtered to remove the silver chloride precipitate and then rotary evaporated down to a volume of approximately 0.5 mL. A volume of 3 mL of 18.2 MΩ·cm water was added, inducing the formation of a precipitate. The suspension was stirred for 3 h and then lyophilized to obtain the product as a fluffy yellow solid (orange in the case of **11**).

NN = bpy (8) (61%). IR (νCO/cm^{-1}): 2035, 1930, 1903. ^{1}H NMR (300 MHz, MeOD-d_4 with 15% D_2O): δ 9.11 (d, 2H); 8.62 (d, 2H); 8.37 (t, 2H); 7.79 (t, 2H). ^{19}F{^{1}H} NMR (376 MHz, MeOD-d_4 with 15% D_2O): δ −79.95 (s, 3F). Anal. Calcd. for [Re(bpy)(CO)$_3$(OTf)] ($Re_1C_{14}H_8F_3N_2O_6S_1$): C, 29.22; H, 1.40; N, 4.87. Found: C, 29.91; H, 1.64; N, 4.89%. ESI-MS (70% MeCN) *m/z* 425.0071, 427.0099 ([Re(bpy)(CO)$_3$]$^+$, calcd 425.0059, 427.0087) *m/z* 443.0178, 445.0206 ([Re(bpy)(CO)$_3$(H$_2$O)]$^+$, calcd 443.0165, 445.0193).

NN = dmbpy (9) (83%). IR (νCO/cm^{-1}): 2035, 1939, 1917. ^{1}H NMR (300 MHz, MeOD-d_4 with 15% D_2O): δ 8.92 (d, 2H); 8.44 (s, 2H); 7.59 (d, 2H); 2.62 (s, 6H). ^{19}F{^{1}H} NMR (376 MHz, MeOD-d_4 with 15% D_2O): δ −79.95 (s, 3F). Anal. Calcd. for [Re(dmbpy)(CO)$_3$(OTf)] ($Re_1C_{16}H_{12}F_3N_2O_8S_1$): C, 31.84; H, 2.00; N, 4.64. Found: C, 31.36; H, 2.34; N, 4.75%. ESI-MS

(70% MeCN) *m/z* 453.0384, 455.0411 ([Re(dmbpy)$(CO)_3]^+$, calcd 453.0372, 455.0400) *m/z* 471.0491, 473.0518 ([Re(dmbpy)$(CO)_3(H_2O)]^+$, calcd 471.0478, 473.0506).

NN = dmobpy (10) (66%). IR (νCO/cm^{-1}): 2030, 1930, 1878. ^{1}H NMR (300 MHz, MeOD-d_4 with 15% D_2O): δ 8.88 (d, 2H); 8.00 (d, 2H); 7.26 (dd, 2H); 4.09 (s, 6H). $^{19}F\{^1H\}$ NMR (376 MHz, MeOD-d_4 with 15% D_2O): δ −79.98 (s, 3F). Anal. Calcd. For [Re(dmobpy)$(CO)_3$(OTf)] ($Re_1C_{16}H_{12}F_3N_2O_6S_1$): C, 30.24; H, 1.90; N, 4.41. Found: C, 29.97; H, 2.11; N, 4.59%. ESI-MS (70% MeCN) *m/z* 485.0283, 487.0310 ([Re(dmobpy)$(CO)_3]^+$, calcd 485.0270, 487.0298) *m/z* 503.0390, 505.0417 ([Re(dmobpy)$(CO)_3(H_2O)]^+$, calcd 503.0376, 505.0404).

NN = diester-bpy (11) (64%). IR (νCO/cm^{-1}): 2030, 1918, 1910, 1726 (ester carbonyl). ^{1}H NMR (300 MHz, $CDCl_3$): δ 9.28 (d, 2H); 8.86 (s, 2H); 8.18 (d, 2H); 4.12 (s, 6H). $^{19}F\{^1H\}$ NMR (376 MHz, MeOD-d_4 with 15% D_2O): δ −79.97 (s, 3F). Anal. Calcd. for [Re(diester-bpy)$(CO)_3(H_2O)$][OTf]·$4H_2O$ ($Re_1C_{18}H_{22}F_3N_2O_{15}S_1$): C, 27.66; H, 2.84; N, 3.58. Found: C, 27.06; H, 2.31; N, 3.83%. ESI-MS (70% MeCN) *m/z* 541.0184, 543.0212 ([Re(diester-bpy)$(CO)_3]^+$, calcd 541.0169, 543.0197) *m/z* 559.0291, 561.0319 [Re(diester-bpy)$(CO)_3(H_2O)]^+$, calcd 559.0274, 561.0302).

NN = phen (12) (63%). IR (νCO/cm^{-1}): 2035, 1930, 1891. ^{1}H NMR (300 MHz, MeOD-d_4 with 15% D_2O): δ 9.51 (d, 2H); 8.94 (d, 2H); 8.30 (s, 2H); 8.13 (dd, 2H). $^{19}F\{^1H\}$ NMR (376 MHz, MeOD-d_4 with 15% D_2O): δ −80.06 (s, 3F). Anal. Calcd. for [Re(phen)$(CO)_3(H_2O)$][OTf]·H_2O ($Re_1C_{16}H_{10}F_3N_2O_7S_1$): C, 31.12; H, 1.63; N, 4.54. Found: C, 31.42; H, 1.81; N, 4.77%. ESI-MS (70% MeCN) *m/z* 449.0073, 451.0100 ([Re(phen)$(CO)_3]^+$, calcd 449.0059, 451.0087) *m/z* 467.0180, 469.0207 [Re(phen)$(CO)_3(H_2O)]^+$, calcd 467.0165, 469.0193).

NN = dmphen (13) (57%). IR (νCO/cm^{-1}): 2030, 1939, 1922. ^{1}H NMR (300 MHz, D_2O with 1,4-dioxane for reference): δ 8.56 (d, 2H); 8.00 (s, 2H); 7.91 (d, 2H); 3.30 (s, 6H). $^{19}F\{^1H\}$ NMR (376 MHz, MeOD-d_4 with 15% D_2O): δ −80.04 (s, 3F). Anal. Calcd. for [Re(dmphen)$(CO)_3(H_2O)$][OTf]·$2H_2O$ ($Re_1C_{18}H_{18}F_3N_2O_9S_1$): C, 31.72; H, 2.66; N, 4.11. Found: C, 31.78; H, 2.23; N, 4.34%. ESI-MS (70% MeCN) *m/z* 477.03896, 479.0414 ([Re(dmphen)$(CO)_3]^+$, calcd 477.0372, 479.0400) *m/z* 495.0493, 497.0520 ([Re(dmphen)$(CO)_3(H_2O)]^+$, calcd 495.0478, 497.0506).

NN = dpphen (14) (61%). IR (νCO/cm^{-1}): 2022, 1939, 1930. ^{1}H NMR (300 MHz, MeOD-d_4 with 15% D_2O): δ 9.56 (d, 2H); 8.21 (s, 2H); 8.09 (s, 2H); 7.69 (m, 10H). $^{19}F\{^1H\}$ NMR (376 MHz, MeOD-d_4 with 15% D_2O): δ −80.03 (s, 3F). Anal. Calcd. for [Re(dpphen)$(CO)_3$(OTf)] ($Re_1C_{28}H_{16}F_3N_2O_6S_1$): C, 44.74; H, 2.15; N, 3.73. Found: C, 44.95; H, 2.61; N, 3.69%. ESI-MS (70% MeCN) *m/z* 601.0702, 603.0730 [Re(dpphen)$(CO)_3]^+$, calcd 601.0685, 603.0713) *m/z* 619.0809, 621.0837 ([Re(dpphen)$(CO)_3(H_2O)]^+$, calcd 619.0791, 621.0819).

Capacity Factor Determination. Capacity factors were determined using HPLC with the column and setup described within the physical measurement section. An isocratic elution of 40% acetonitrile (MeCN) and 60% H_2O (both solvents contained 0.1% TFA) was used at a flow rate of 1 mL/min. The rhenium complexes were dissolved in 50:50 MeCN:water prior to analysis. Two peaks were present in the chromatogram of all complexes; the lower retention time peak corresponds to the more hydrophilic aqua complex and the higher retention time peaks corresponds to the acetonitrile adduct. The dead time of the column was determined using a solution of thiourea, a compound that has no affinity for the RP column.

Radiolabeling. Synthesis of **13*** involved the initial synthesis of technetium tricarbonyl precursor, *fac*-[^{99m}Tc$(H_2O)_3(CO)_3]^+$. Sodium pertechnetate, Na[$^{99m}TcO_4$], was eluted from a

^{99}Mo/^{99m}Tc sterile generator as a 1.0 mL saline solution (0.9% v/v) and provided by Triad Isotopes (Triad Isotopes - Canton, MA). The radioactive solution was then added to a sealed Isolink vial (Paul Scherrer Institute) and heated for 40 min at 100 °C using an oil bath. The solution was cooled to room temperature. A separate solution of the dmphen ligand in ethanol/water (5% EtOH) was prepared (1 mg/mL). To the aqueous *fac*-$[^{99m}Tc(H_2O)_3(CO)_3]^+$ solution (1 mL) was added 1 M HCl (140 μL) to adjust the pH to 7. A 500 μL aliquot was removed and mixed with stock solution of the dmphen ligand (100 μL). The mixture was heated to 60 °C for 60 min under vigorous stirring in a sealed reaction vessel. The reaction was analyzed using analytical radioHPLC. For purification of the radiochemical complex, the reaction mixture was diluted with water (2 mL), and the solution was loaded onto a Waters C18 Sep-Pak light cartridge, which had been previously activated with EtOH (6 mL) and H_2O (12 mL). Unreacted ^{99m}Tc, which may include *fac*-$[^{99m}Tc(H_2O)_3(CO)_3]^+$ and $[TcO_4]^-$, was washed off the column with additional water (20 mL). The radiolabeled product was eluted from the cartridge with ethanol (2 mL). Alternatively, the product can be isolated by collection of the product fraction using preparative radioHPLC, followed by removal of organic solvent in vacuo. **13*** was then reconstituted in 20% ethanol/water. **13*** was isolated with a purified, non-decay corrected yield of 17%. R_t –**13**: 16.8 min (method 3) R_t –**13***: 16.9 min (method 3).

X-ray Crystallography. Crystal data and structure refinement information is given in Tables S3-S6. The crystals were mounted on a Bruker X8 Kappa diffractometer coupled to an ApexII CCD detector with graphite-monochromated Mo Kα radiation (λ = 0.71073 Å) and cooled to 223 K under a nitrogen cold-stream during data collection. The program SHELXT was used to solve the structures via intrinsic phasing,[3] which were refined on all data by full-matrix least squares with SHELXL.[4] Non-hydrogen atoms were refined anisotropically. Hydrogen atoms were placed at calculated positions using a riding model, and were refined isotropically with thermal displacement parameters constrained to be either 1.2 or 1.5 (for terminal CH_3) times that of the atom to which it's attached. Yellow crystals of **11** and orange crystals of **13** were obtained by the vapor diffusion of diethyl ether into acetone solutions. The analogues $[Re(dmbpy)(CO_3)(H_2O)][NO_3]$ (**9**-NO_3) and $[Re(dmobpy)(CO_3)(H_2O)][BF_4]$ (**10**-BF_4) were prepared as described for the triflate salts by substituting $AgNO_3$ or $AgBF_4$ for AgOTf. Yellow crystals of **9**-NO_3 formed from vapor diffusion of hexane into an acetone solution, and yellow crystals of **10**-BF_4 formed from vapor diffusion of diethyl ether into an acetonitrile solution.

Cell Culture. Cells were cultured in a humidified incubator at 37 °C with 5% CO_2. HeLa and MRC-5 cells were obtained from America Type Culture Collection, KB-3-1 and KBCP20 cell lines[5,6] were obtained from the Laboratory of Cell Biology at the National Cancer Institute (Bethesda, MD, USA), and A2780 and A2780CP70 cell lines[7] were obtained from the Cell Culture Facility of Fox Chase Cancer Center (Philadelphia, PA, USA). A549, A549 CisR, H460, and H460 CisR cell lines[8] were obtained from the Thoracic Oncology Research Group (Dublin, Ireland). HeLa, KB-3-1, KBCP20 cells were cultured as monolayers in Dulbecco's Modified Eagle Medium (DMEM) supplemented with 10% fetal bovine serum (FBS). Medium for growth of the KB cells also contained 1 mM sodium pyruvate. A2780 and A2780CP70 cells were cultured with RPMI medium (Roswell Park Memorial Institute) containing 10% FBS and 69 μU/mL insulin. MRC-5 cells were grown in Minimal Essential Medium (MEM) with 10% FBS. A549 and A549 CisR cells were cultured in Ham's medium containing 10% FBS. H460 and H460 CisR cells were grown in RPMI medium containing 10% FBS. Cells were routinely passed at 80–90% confluence, using

trypsin/EDTA. Cells were tested monthly for mycoplasma contamination with the PlasmoTest™ mycoplasma detection kit from InvivoGen.

Viability Assays. Stock solutions of the rhenium complexes were prepared in pure 18.2 MΩ·cm water except for **14** which was prepared as a 5% DMSO solution. Cells were seeded in a 96-well plate at a density of 2000 cells/well. After 24 h, the growth medium was removed and replaced with 200 µL of growth medium containing varied concentrations of the complexes of interest. After an additional 72 h incubation, the medium was removed and replaced with 200 µL of 5 mg/mL 3-(4,5-dimethylthiazol-2-yl)-2,5-diphenyltetrazolium bromide (MTT), diluted in serum-free medium. After 4–8 h, the MTT was removed, and the resulting purple formazan crystals were dissolved in 200 µL DMSO containing 17% 0.1 M glycine and 0.1 M NaCl at pH 10.5. The absorbance at 570 nm in each well was determined using a BioTek Synergy HT plate reader. Six replicates per concentration level and at least three independent experiments were completed for each compound. The data points were fit to the equation:[9] $y = E_{inf} + ((E_0-E_{inf})/(1+(D/IC_{50})^{HS}))$; where y is the viability, E_{inf} is the viability at infinite drug concentration, E_0 is the viability at zero drug concentration, D is the drug concentration, IC_{50} is the 50% growth inhibitory concentration, and HS is the Hill slope, a measure of the steepness of the resulting dose-response curve. E_{inf} was constrained to lie between 0 and 0.05, and E_0 was constrained to lie between 0.95 and 1. The variables E_{inf}, E_0, IC_{50}, and HS were fit using MagicPlot to best match the experimental data.

Nucleobase and Amino Acid Binding. Solutions were prepared in 1:1 MeOH:buffer that were 500 µM in **13** and 10 mM in substrate at room temperature (21 °C). The buffer solution was prepared as 100 mM MOPS buffer adjusted to pH 7.3. At the indicated time points, a 5 µL sample of the reaction mixture was analyzed by analytical HPLC. The HPLC method was the same as described under Physical Measurements.

Cell Cycle Analysis. HeLa cells were grown for the indicated time in medium or medium with a compound of interest. Approximately 1×10^6 cells were used for each trial. The cells were harvested and centrifuged, and then the supernatant was discarded. A volume of 1 mL 70% ethanol at 4 °C was added and the cells were resuspended. The cells were fixed at 4 °C for 30 min and then centrifuged. The cells were kept at 4 °C until the day of analysis, which was always within one week. The cells were resuspended in phosphate buffered saline (PBS) and washed by centrifuging, removing the supernatant, and resuspending in PBS. A 50 µL portion of a 100 µg/mL solution of ribonuclease A and 20 µL of a 1 mg/mL solution of propidium iodide were then added to the cells in 200 µL PBS. The cells were then analyzed for propidium iodide fluorescence using a Beckman-Coulter XL flow cytometer. The histogram was curve fit with four curves in MagicPlot to determine the percentage of cells in each phase of the cell cycle. The S phase was fit with a modified super Gaussian function: $y = g(e^{\wedge}(-2((x-c)/R)^p))$; where y is the cell count, g is the maximum cell count, x is the PI fluorescence intensity, c is the mean PI intensity in the S phase, R is half the width, and p is the order parameter which affects the shape of the sides of the curve. The three remaining cell phase groups were fit with Gaussian curves.

ROS Analysis. Approximately 1×10^5 cells were used for each trial. HeLa cells were grown under the indicated conditions, and then the medium was replaced with medium containing 10 µM 2′,7′-dichlorofluorescin diacetate for 30 min. The cells were washed by centrifuging, removing the

supernatant, and resuspending in PBS. The cells were then analyzed for 2′,7′-dichlorofluorescein fluorescence by flow cytometry.

Annexin V/PI Assay. The reported protocol was followed for HeLa cells.[10] In brief, HeLa cells were grown under the indicated conditions, and then the cells were centrifuged, the supernatant was removed, and the cells were resuspended in Annexin V binding buffer. Next, 5 µL Annexin V-Alexa Fluor 488 and 4 µL of 0.1 mg/mL propidium iodide solution were added. The cells were fixed in 1% formaldehyde on ice and then suspended in 15 µg/mL RNase in PBS at 37 °C. The cells were then analyzed by flow cytometry for propidium iodide and Alexa Fluor 488 fluorescence.

JC-1 Assay. HeLa cells were grown under the indicated conditions, and then the cells were washed by centrifuging, removing the supernatant, and resuspending in 150 µL PBS. A 12.5 µL portion of 40 µM JC-1 was added to each tube. A control tube was treated with 300 µM CCCP as positive control. After 15 min, 150 µL PBS was added and the cells were analyzed for JC-1 green monomers and red aggregates by flow cytometry.

Western Blotting. HeLa cells were grown under the indicated conditions, and then collected and lysed in SDS lysis buffer. Equal concentrations of protein were loaded into each gel lane, as determined by the BCA assay, and after separation the proteins were transferred to a polyvinylidene difluoride (PVDF) membrane. The membrane was treated with blocking solution, followed by primary and then HRP-conjugated secondary antibodies. The ECL reagents were mixed and added to the membrane, and the membrane was imaged with a GE Typhoon 7000 scanner.

Uptake by Flow Cytometry. HeLa cells were grown under the indicated conditions, and then washed by centrifuging, removing the supernatant, and resuspending in 200 µL PBS. For cells that were analyzed for viability, 2 µL of a 1 mg/mL solution of propidium iodide was added. The cells were analyzed by flow cytometry for rhenium tricarbonyl diimine luminescence (using 405 nm excitation and 610/20 nm emission) and propidium iodide fluorescence if required.

Fluorescence Microscopy. HeLa cells (1×10^5) were seeded on a 35 mm dish with a microscope cover slide one day in advance. The cells were treated as indicated, and then the medium was replaced with an imaging buffer (20 mM HEPES pH 7.4, 135 mM NaCl, 5 mM KCl, 1.8 mM $CaCl_2$, 1 mM $MgCl_2$, 1 mg/mL glucose, and 1 mg/mL BSA). The cells were then imaged with a Zeiss LSM 800 or Zeiss LSM 880 confocal laser scanning microscope. The rhenium complexes were imaged using 405 nm excitation and a 475–700 nm emission filter, and images were processed with the ImageJ software. For transfections, a solution of 2 µL Lipofectamine 2000 in 150 µL Transfectagro was prepared for each dish. In a separate tube, 1 µg of plasmid DNA was diluted to 150 µL of Transfectagro. After 5 min, the two solutions were mixed, and after 20 min, they were added to the cells in 2 mL Transfectagro with 10% FBS. After 3 h, the Transfectagro was replaced with regular growth medium (DMEM with 10% FBS), and the cells were imaged 1–2 days later with the indicated treatment. For Hoechst 33342 treatment, 1 µL of 16 mM dye was added to 2 mL of medium 10 min prior to imaging. For LysoTracker Red DND-99 treatment, 1 µL of 100 µM dye was added to 2 mL of medium 2 h prior to imaging.

Biodistribution. All animal experiments were conducted according to the guidelines of the Institutional Animal Care and Use Committee (IACUC). Healthy, female C57/Bl6 mice (10 weeks old, Charles River Laboratories, Cambridge, MA) were intravenously injected simultaneously with 10–25 µCi of **13*** and 0.2 µmol **13** through a tail vein catheter. Mice were sacrificed at 30 min, 60 min, 120 min, or 24 h post injection (n = 3–4 per time point). The following organs were harvested and collected: Blood (obtained via cardiac puncture), heart, liver, kidney, ovary, muscle (thigh), bone (femur), urine; for technetium, radioactivity was counted using a gamma counter. Radioactivity associated with each organ was expressed as percent injected dose per gram (% ID/g). For rhenium, organs were frozen, stored at least overnight to allow for decay of the ^{99m}Tc, defrosted, and transferred to scintillation vials. Nitric acid (3 mL) was added, the vials were sealed and the organs were left to digest for 20 hours at 37 °C. 300 µL of organ digest was diluted with 3 mL of ICP diluent and subsequently analyzed for ^{187}Re content using ICP. % ID/g was calculated based on injection volumes used for each animal (ranging from 0.16–0.22 µmol per mouse; on average, the administered Re dose was 10 µmol/ kg with 0.2 µmol/mouse).

Blood Metabolite Analysis. Blood and urine were collected during organ harvest and stored frozen during decay of ^{99m}Tc. Blood was centrifuged at 2000g to separate plasma. Plasma (100 µL) was decanted and mixed with acetonitrile (100 µL) to precipitate plasma proteins. The mixture was vortexed for 30 seconds and subsequently centrifuged. The supernatant was removed and transferred for direct injection and chromatographic separation via HPLC. Urine (50 µL) was diluted with water (100 µL) and transferred for direct injection and detection of ^{187}Re via LC-ICP-MS using method 2.

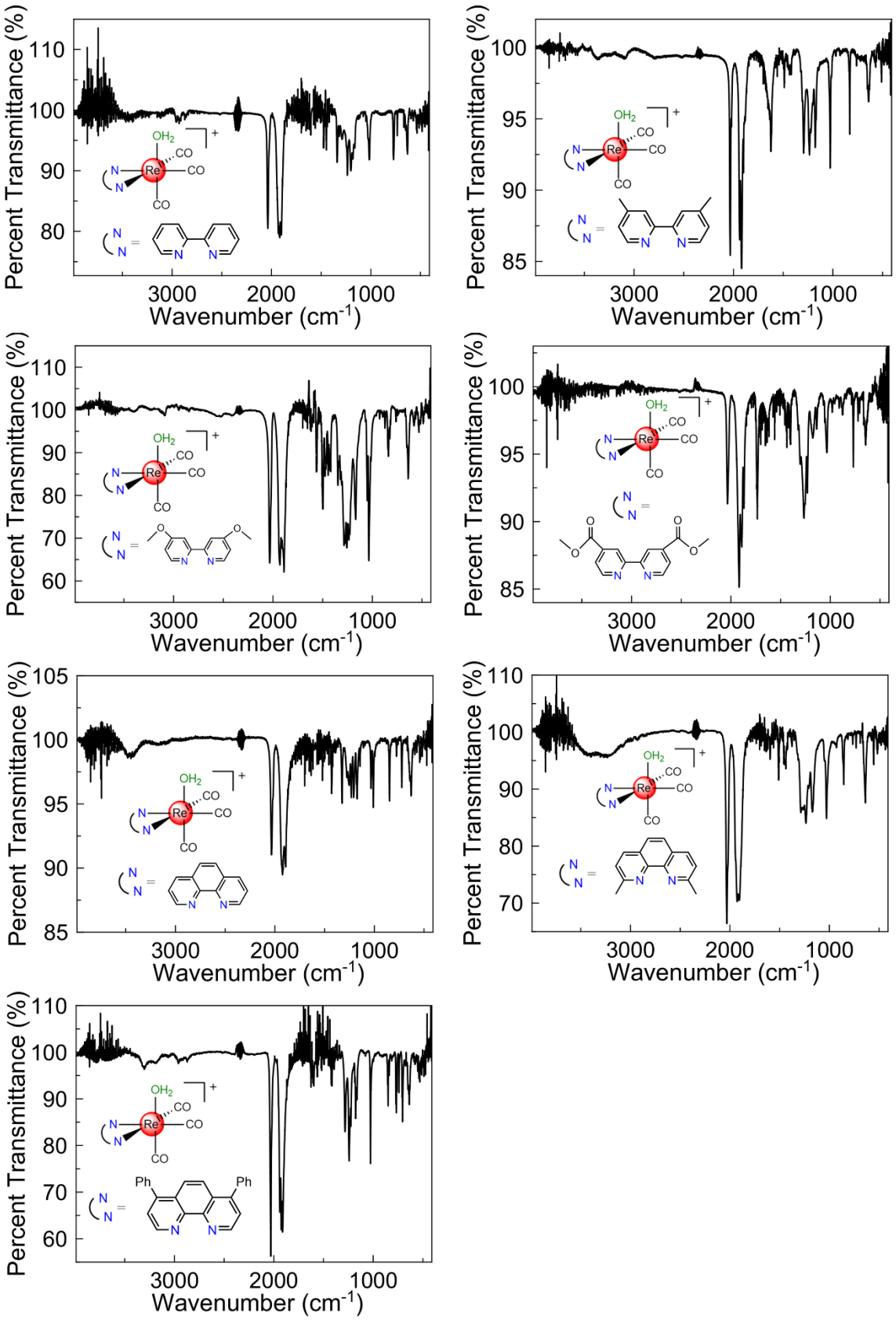

Figure S1. Infrared spectra of **8**–**14**.

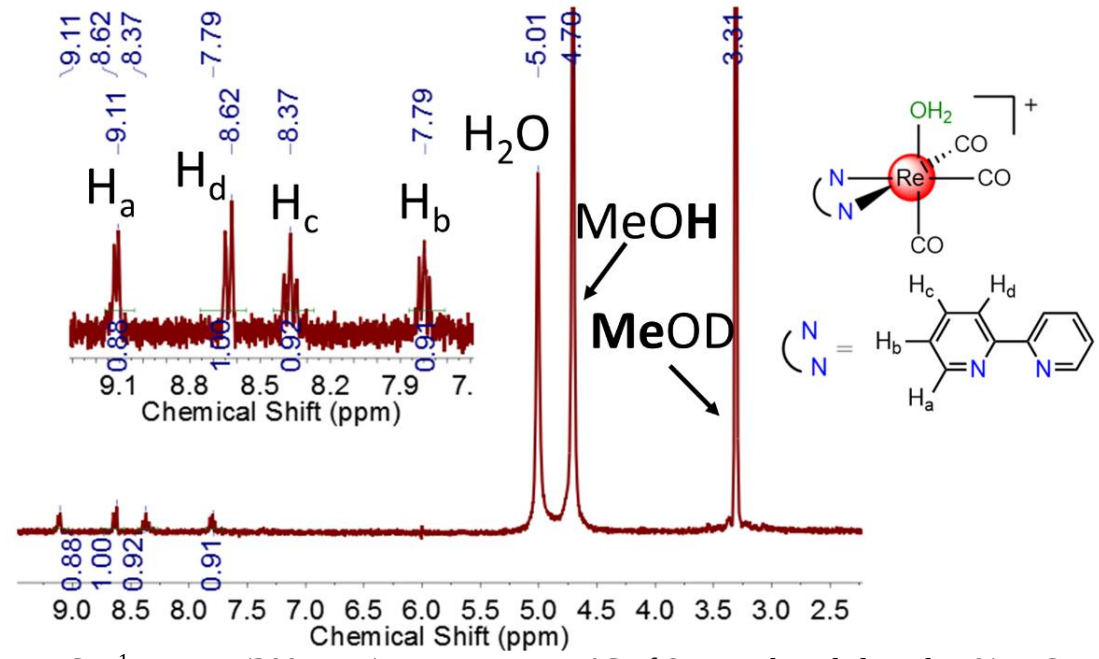

Figure S2. ^{1}H NMR (300 MHz) spectrum at 21 °C of **8** in methanol-d_4 and 15% D_2O.

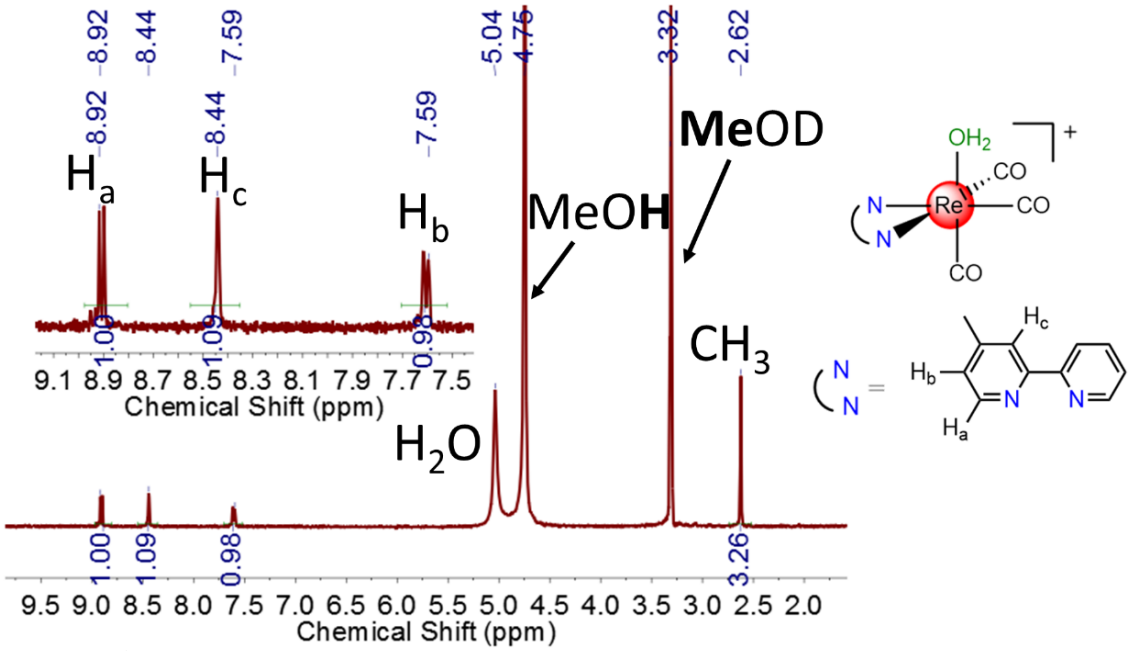

Figure S3. ^{1}H NMR (300 MHz) spectrum at 21 °C of **9** in methanol-d_4 and 15% D_2O.

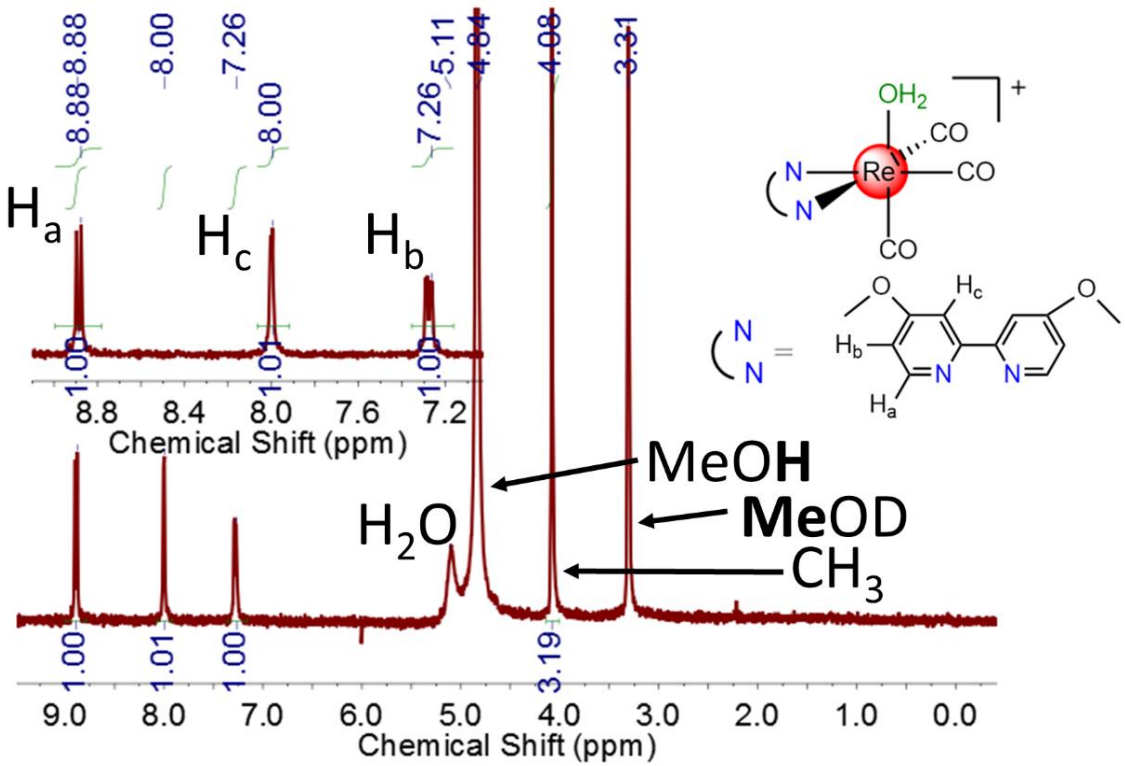

Figure S4. ^{1}H NMR (300 MHz) spectrum at 21 °C of **10** in methanol-d_4 and 15% D_2O.

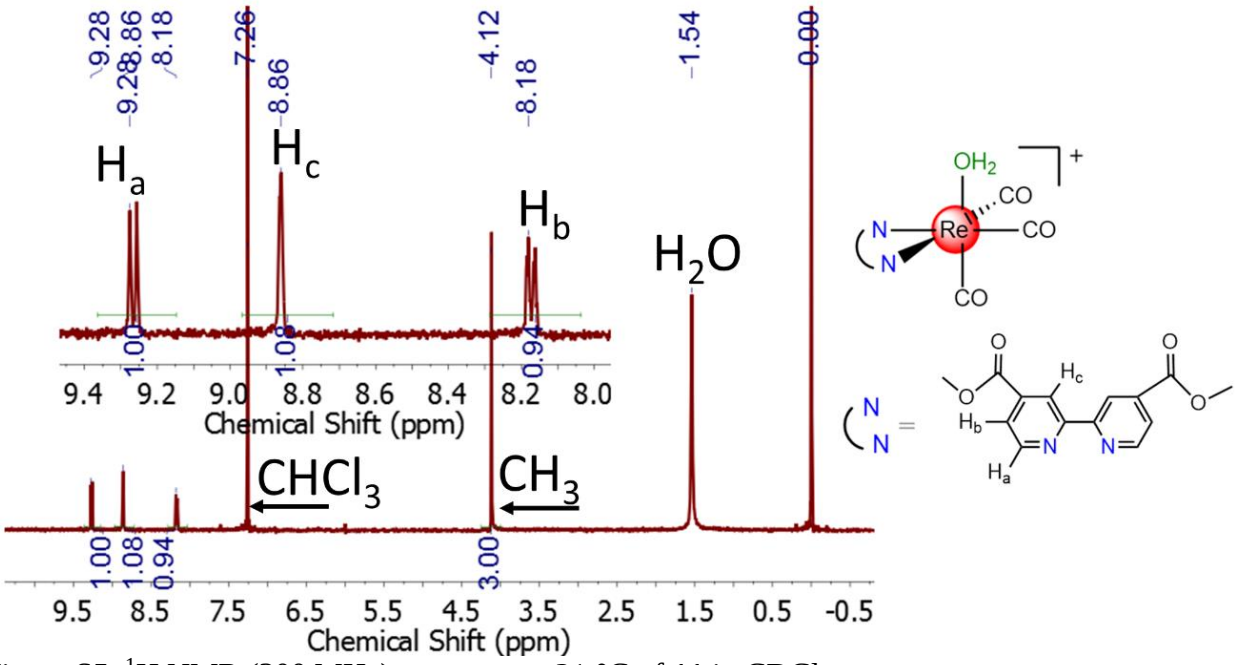

Figure S5. ^{1}H NMR (300 MHz) spectrum at 21 °C of **11** in $CDCl_3$.

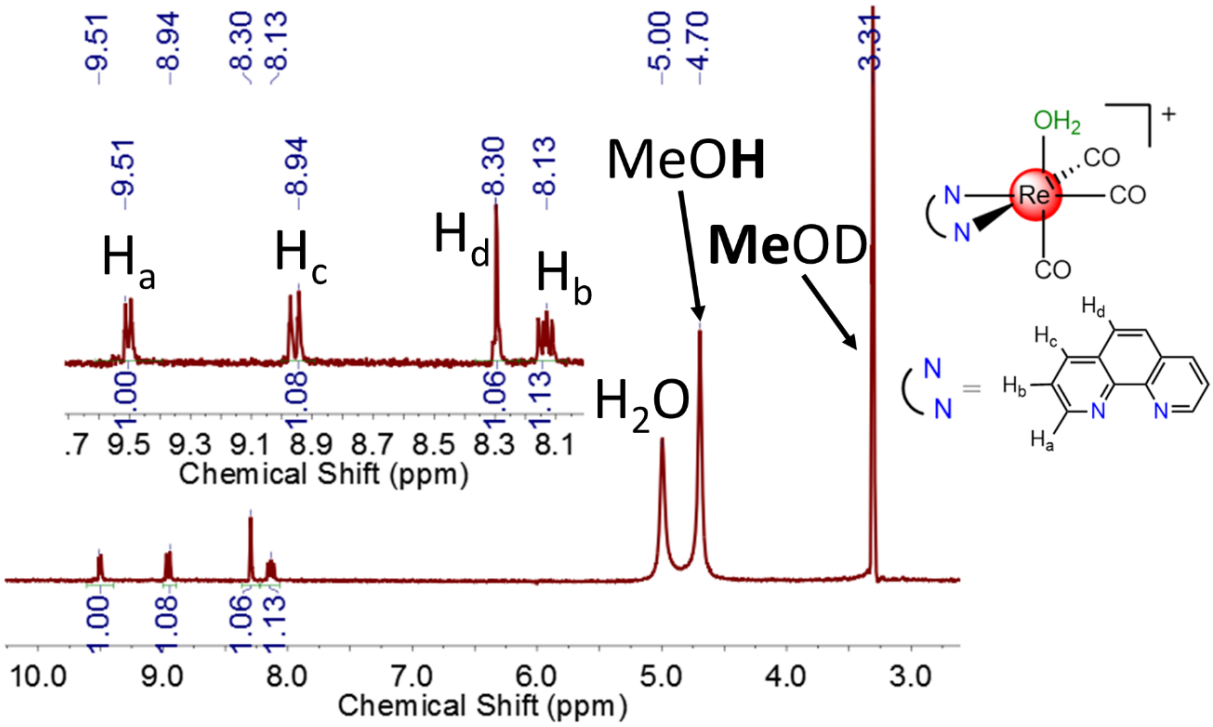

Figure S6. ^{1}H NMR (300 MHz) spectrum at 21 °C of **12** in methanol-d_4 and 15% D_2O.

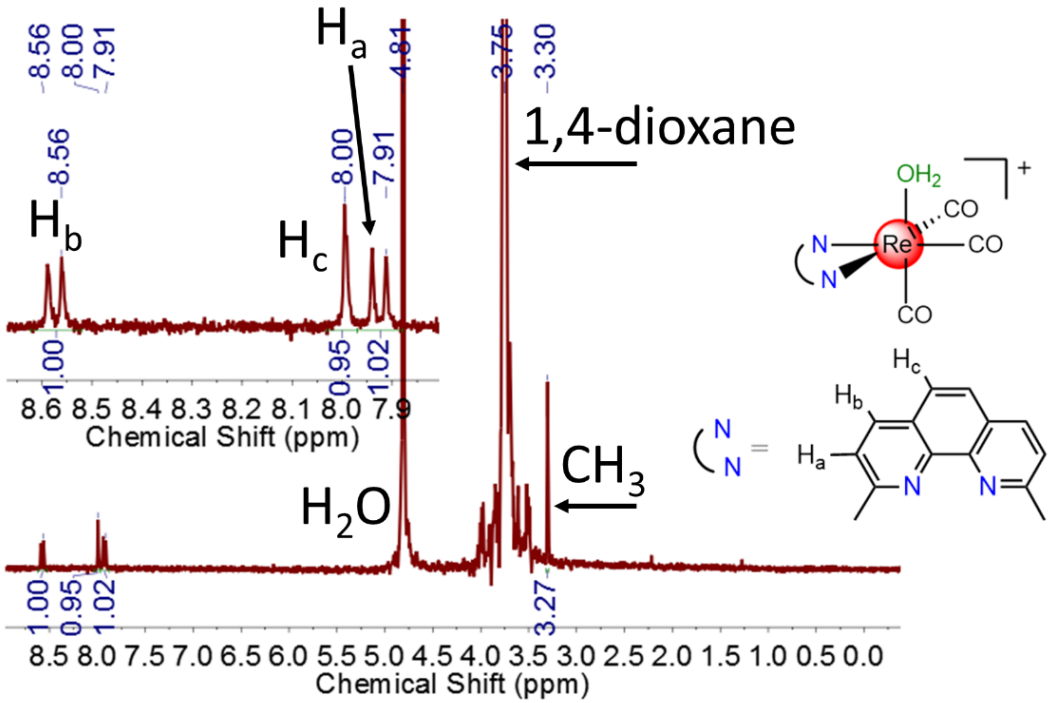

Figure S7. ^{1}H NMR (300 MHz) spectrum at 21 °C of **13** in D_2O with added 1,4-dioxane for reference.

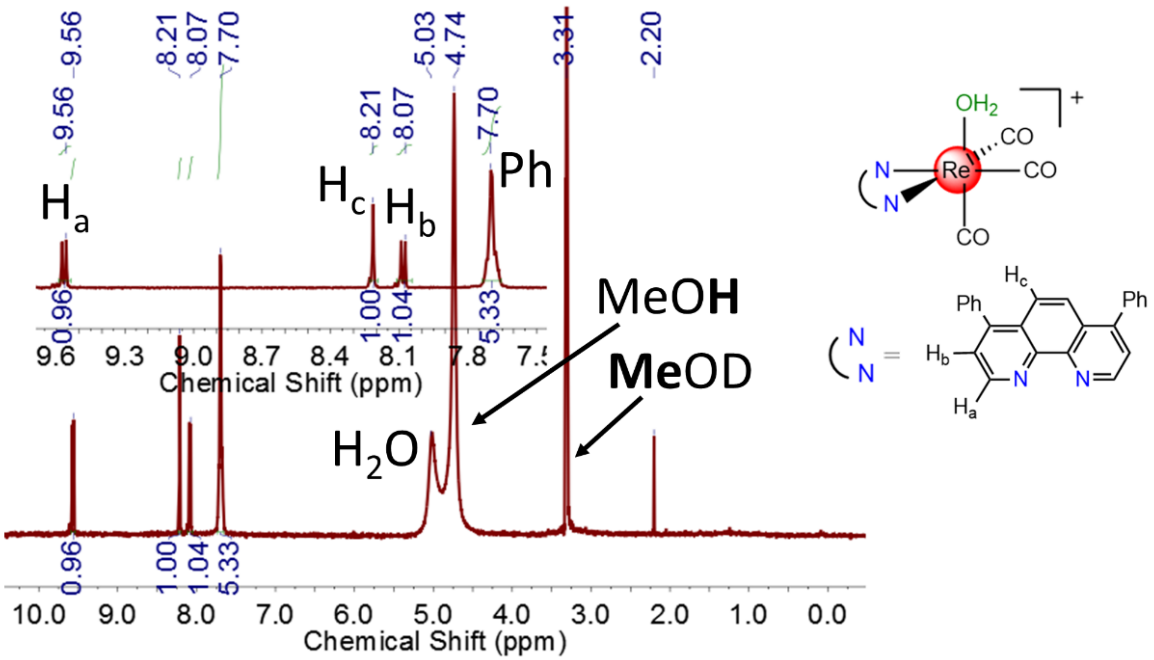

Figure S8. ^{1}H NMR (300 MHz) spectrum at 21 °C of **14** in methanol-d_4 and 15% D_2O.

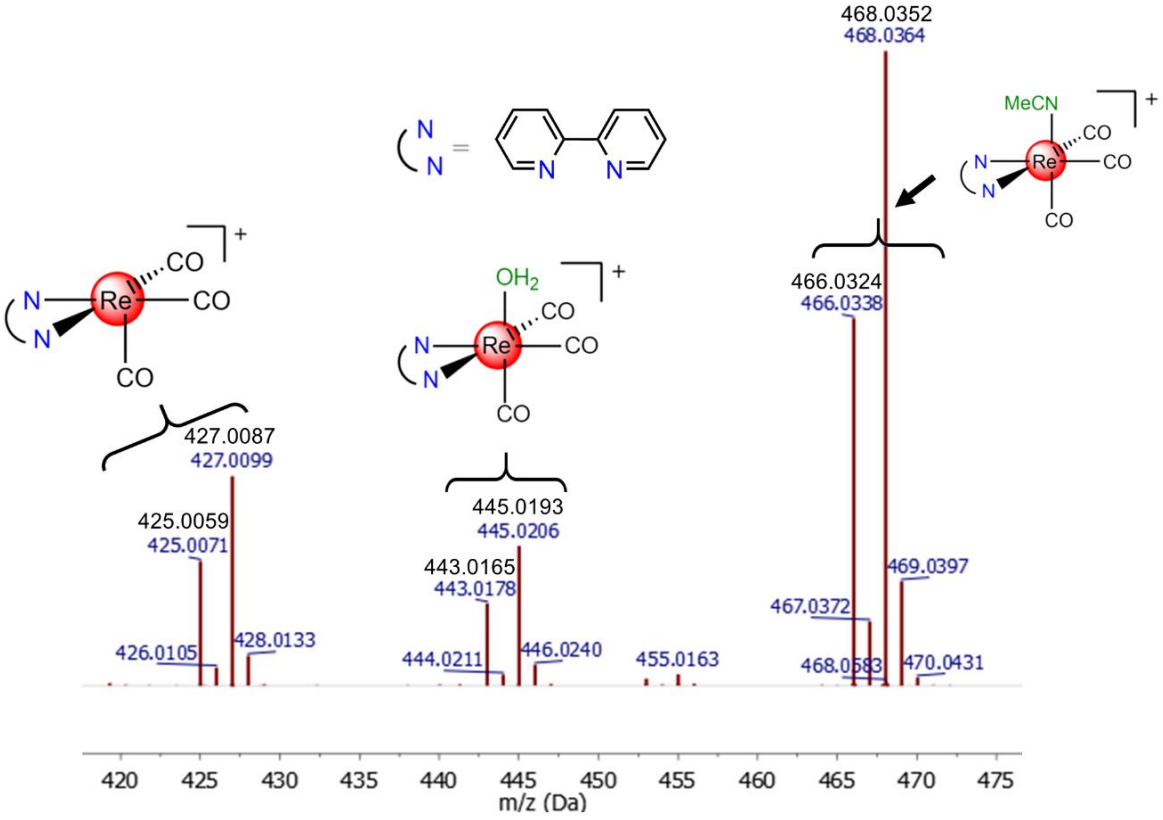

Figure S9. ESI-MS of **8** (70% MeCN). Calculated values are shown in black.

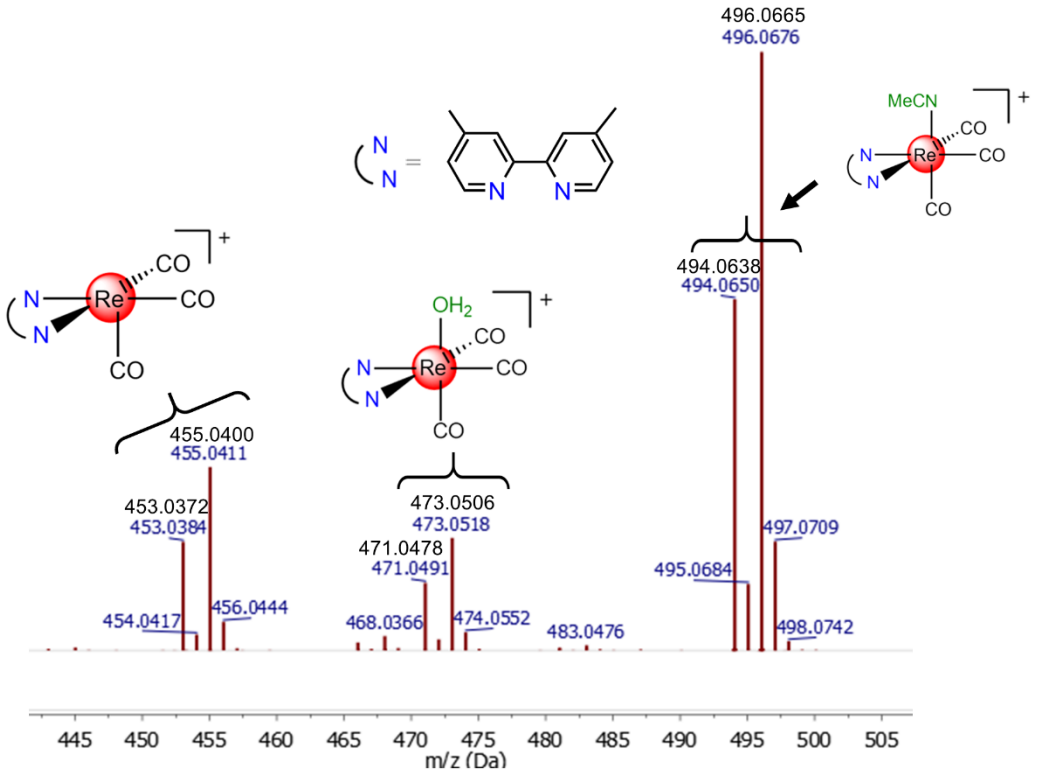

Figure S10. ESI-MS of **9** (70% MeCN). Calculated values are shown in black.

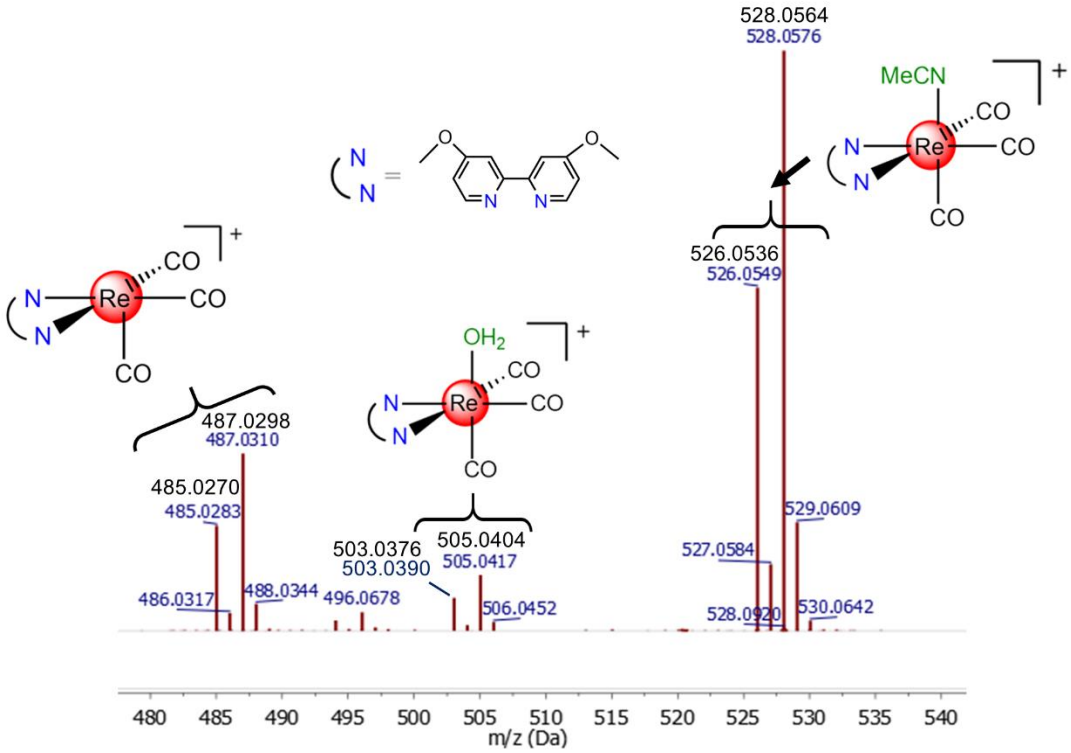

Figure S11. ESI-MS of **10** (70% MeCN). Calculated values are shown in black.

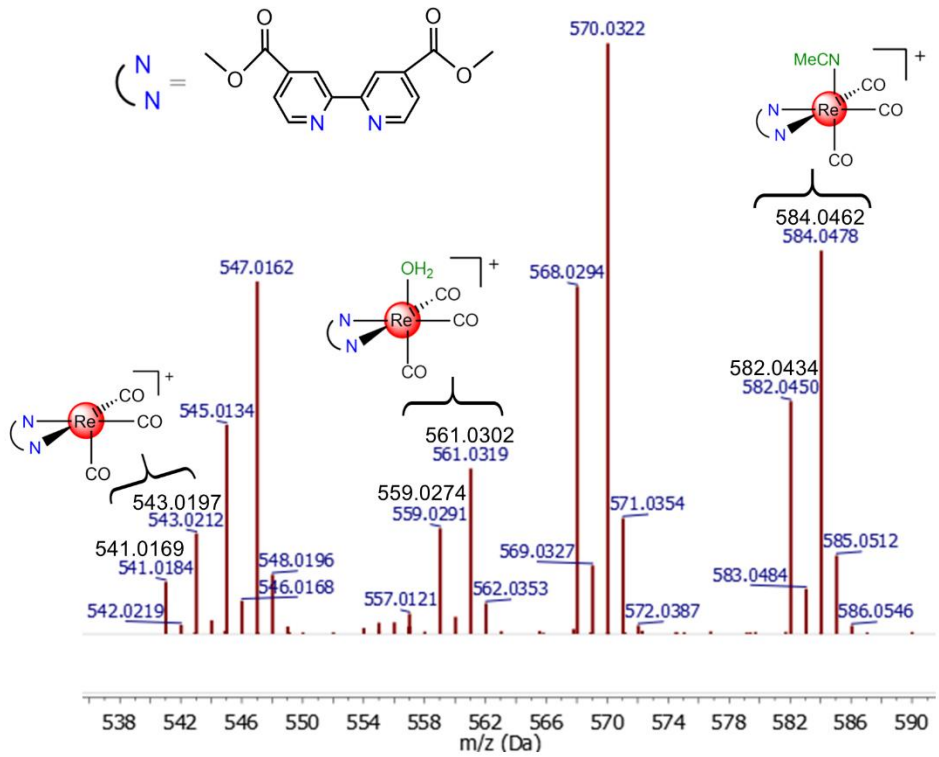

Figure S12. ESI-MS of **11** (70% MeCN). Calculated values are shown in black.

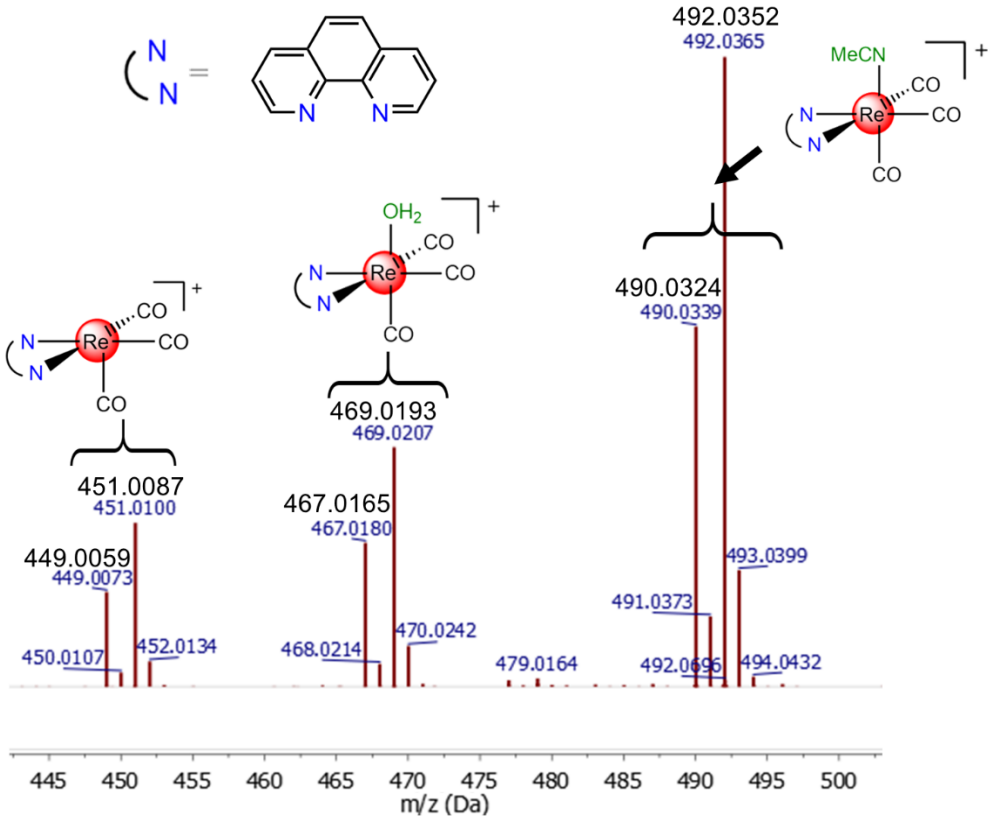

Figure S13. ESI-MS of **12** (70% MeCN). Calculated values are shown in black.

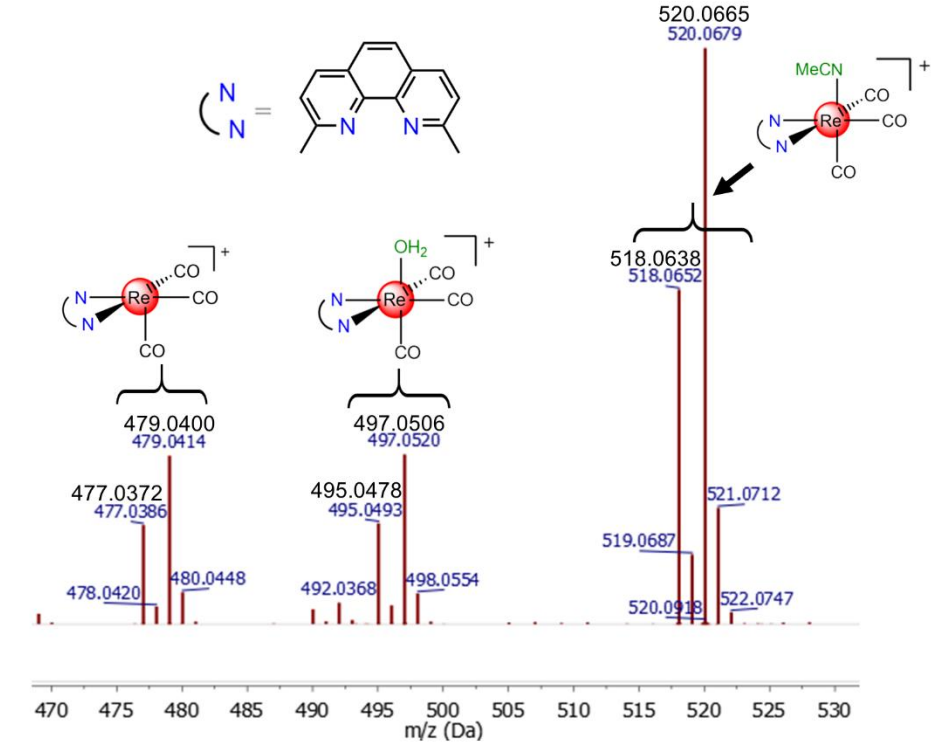

Figure S14. ESI-MS of **13** (70% MeCN). Calculated values are shown in black.

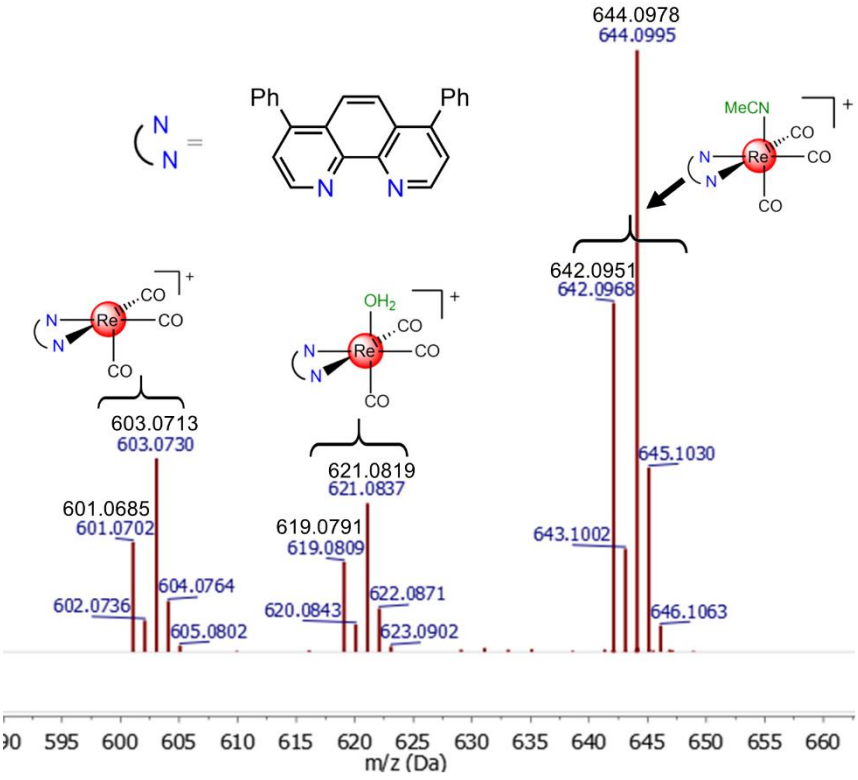

Figure S15. ESI-MS of **14** (70% MeCN). Calculated values are shown in black.

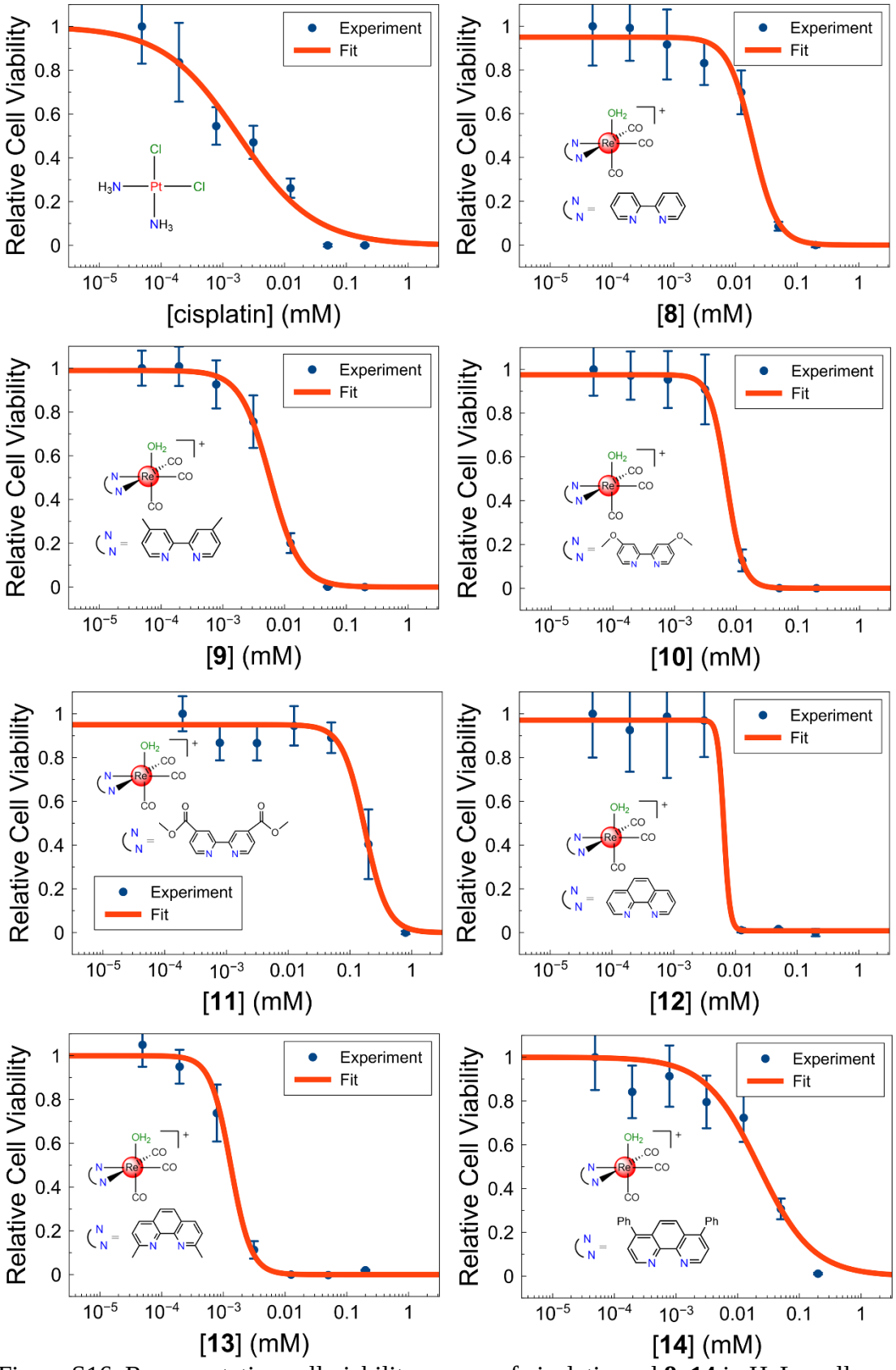

Figure S16. Representative cell viability curves of cisplatin and **8**–**14** in HeLa cells.

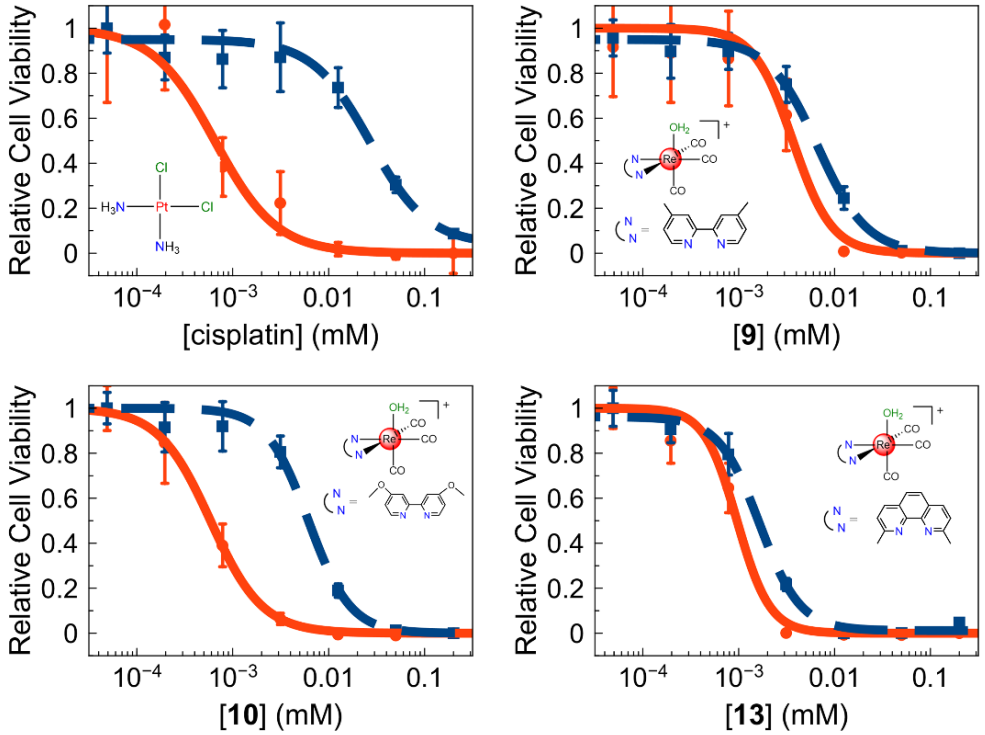

Figure S17. Representative cell viability curves of cisplatin, **9, 10,** and **13** in KB-3-1 (red circles, solid line) and KBCP20 (blue squares, dashed line) cells.

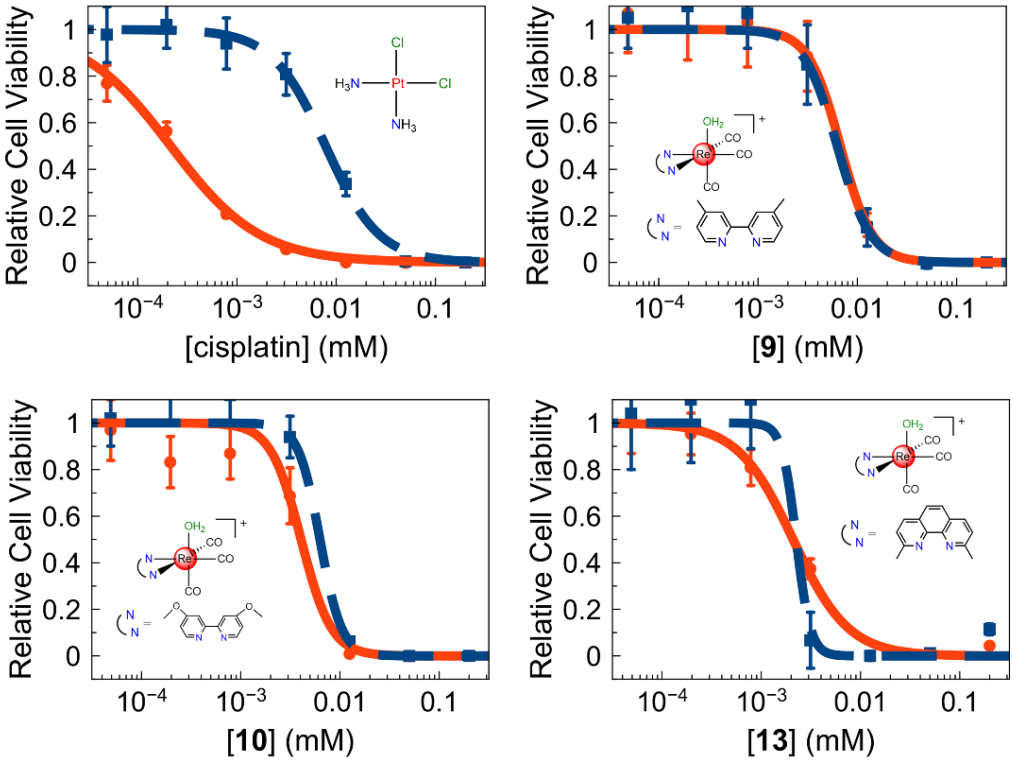

Figure S18. Representative cell viability curves of cisplatin, **9, 10,** and **13** in A2780 (red circles, solid line) and A2780CP70 (blue squares, dashed line) cells.

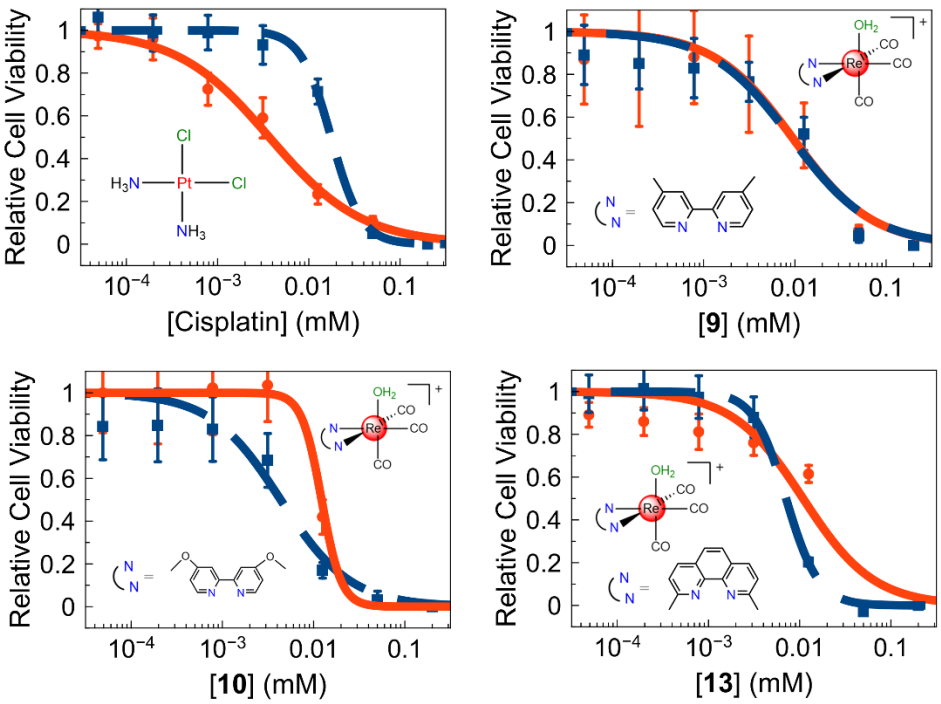

Figure S19. Representative cell viability curves of cisplatin, **9, 10,** and **13** in A549 (red circles, solid line) and A549 CisR (blue squares, dashed line) cells.

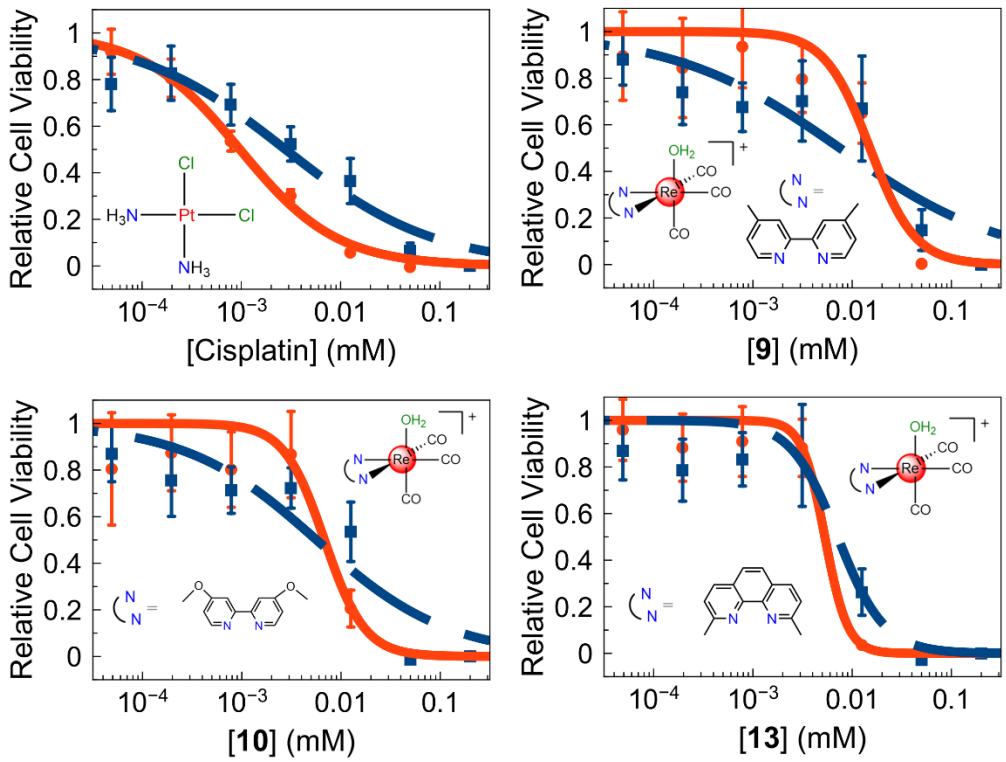

Figure S20. Representative cell viability curves of cisplatin, **9, 10,** and **13** in H460 (red circles, solid line) and H460 CisR (blue squares, dashed line) cells.

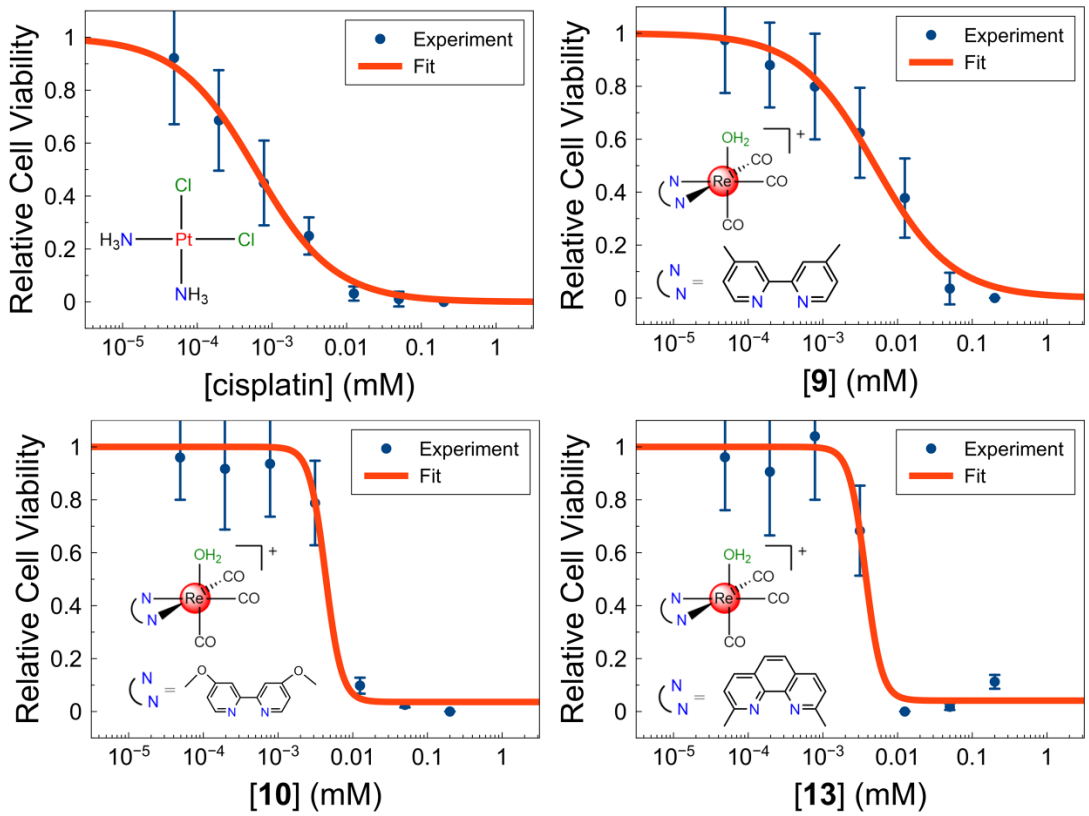

Figure S21. Representative cell viability curves of cisplatin, **9, 10,** and **13** in MRC-5 cells.

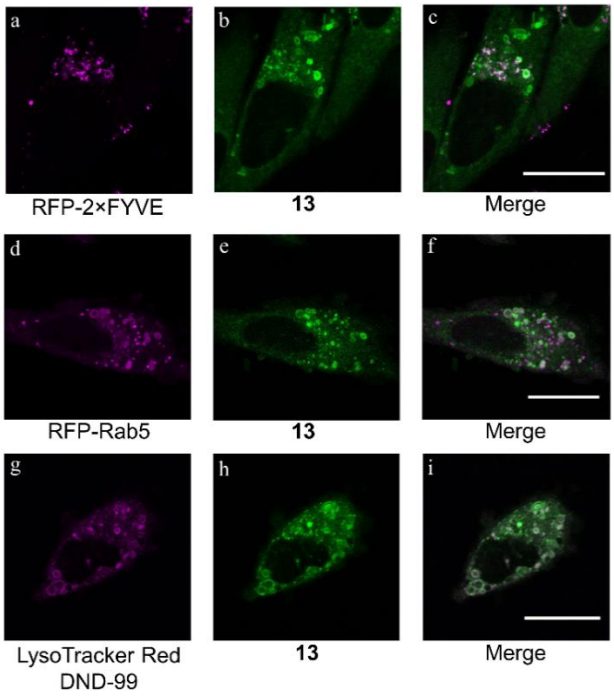

Figure S22. Confocal fluorescent microscope images of HeLa cells treated with **13** (25 μM for 4 h). Cells were additionally stained with the indicated transfection or dye. Scale bars = 20 μm.

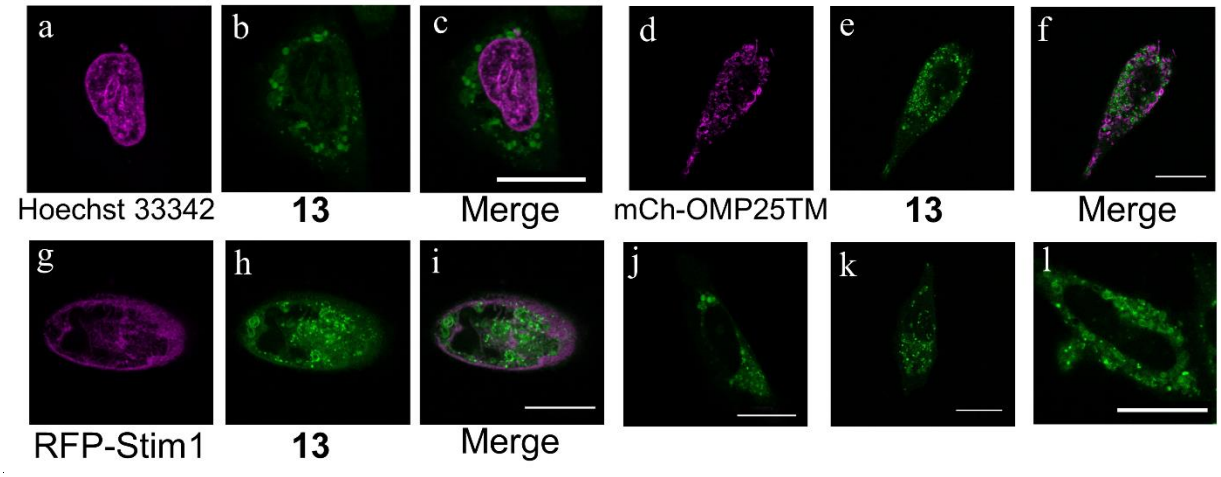

Figure S23. Confocal fluorescent microscope images of HeLa cells treated with 25 µM **13** for 4 h. Cells were additionally stained with a–c) Hoechst 33342 [a) nuclei, b) **13**, c) overlay], d–f) mCh-OMP25TM transfection [d) mitochondria, e) **13**, f) overlay], or g–i) RFP-Stim1 transfection [g) endoplasmic reticulum, h) **13**, i) overlay]. Cells were additionally cultured with j) 1 µM cycloheximide, k) 20 µM 2-aminoethoxydiphenyl borate, or l) 100 µM 3-methyladenine. Scale bars = 20 µm.

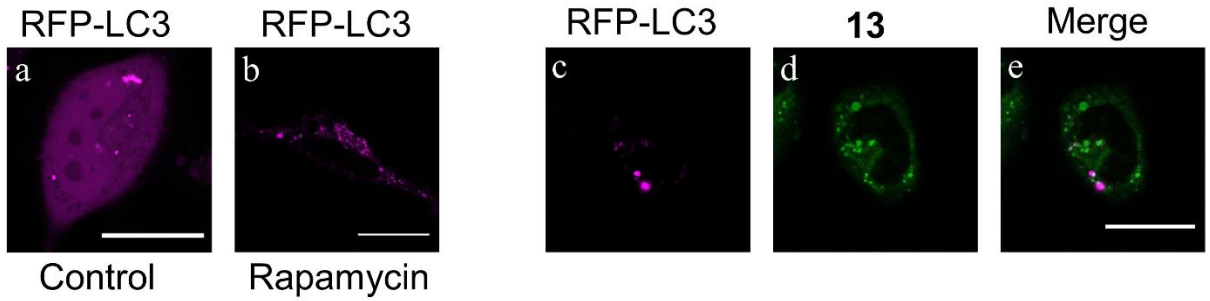

Figure S24. Confocal fluorescent microscope images of HeLa cells transfected with RFP-LC3. Cells were treated with a) no additional treatment, b) 50 µM rapamycin for 4 h as positive control, or c–e) 25 µM **13** for 4 h. Scale bars = 20 µm.

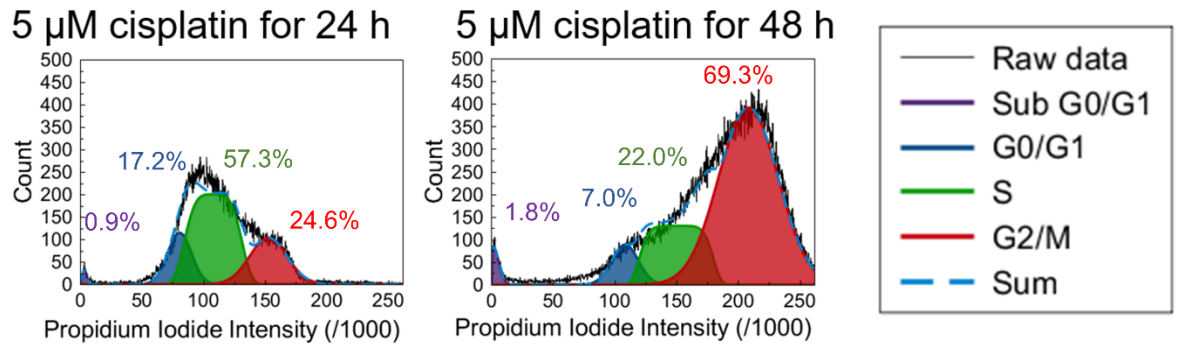

Figure S25. Cell cycle analysis of HeLa cells treated with cisplatin.

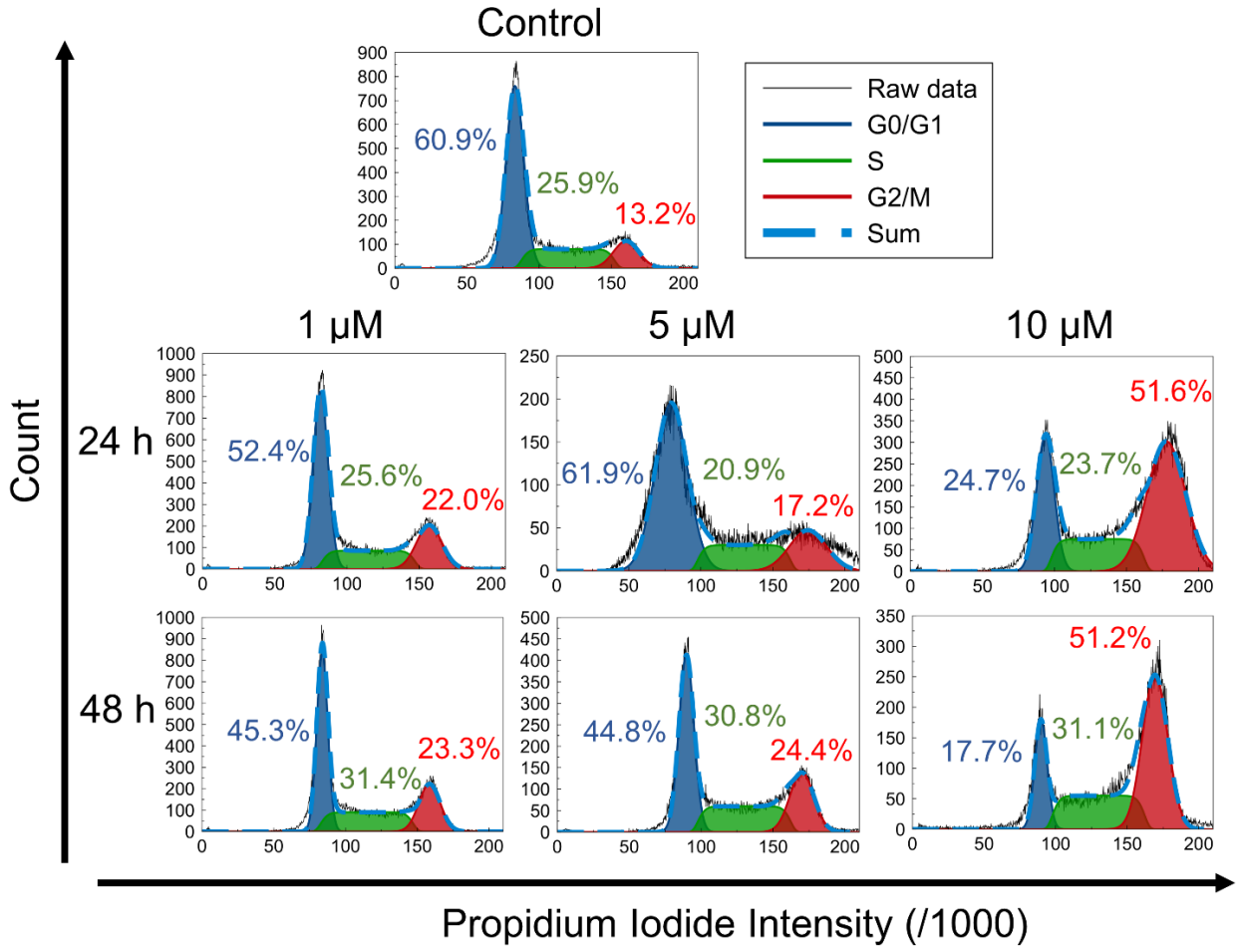

Figure S26. Cell cycle analysis of control HeLa cells, or in the presence of **13** at the indicated concentrations and times.

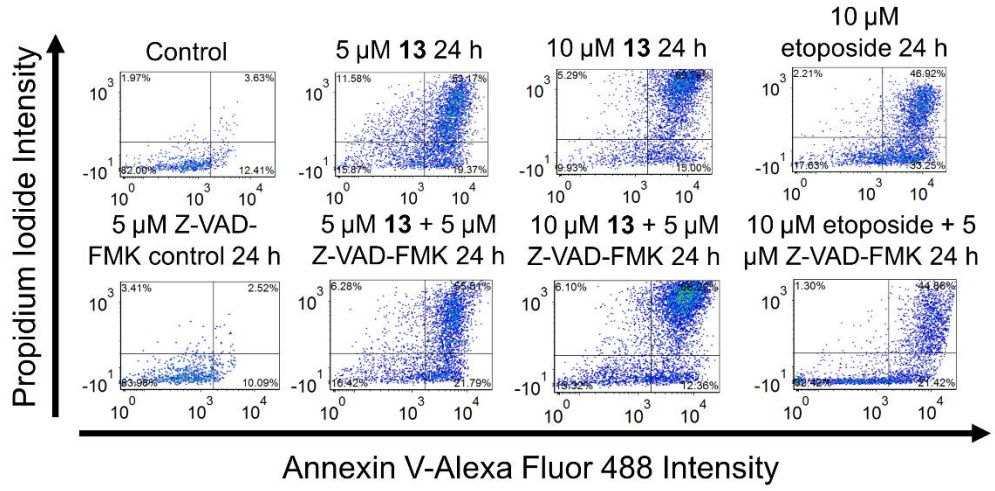

Figure S27. Annexin V/PI assay of HeLa cells treated with **13**, etoposide, and/or the pan-caspase inhibitor Z-VAD-FMK for 24 h.

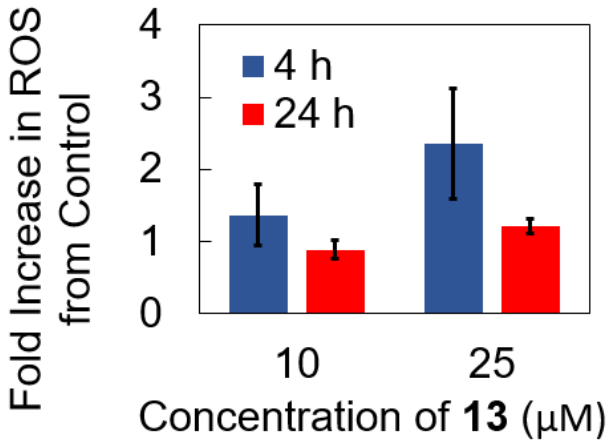

Figure S28. ROS levels in HeLa cells treated with **13**. Error bars represent one standard deviation.

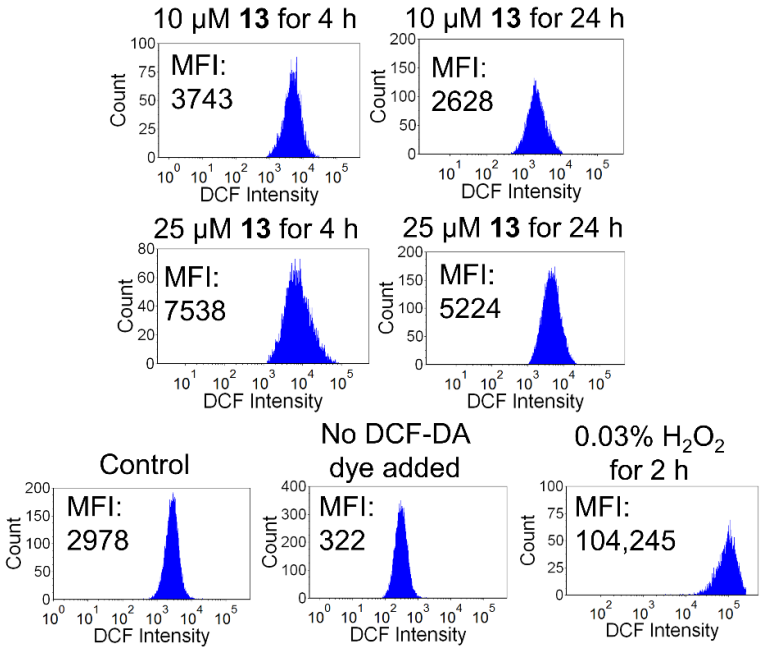

Figure S29. Representative histograms for the analysis of ROS by flow cytometry. MFI = mean fluorescence intensity.

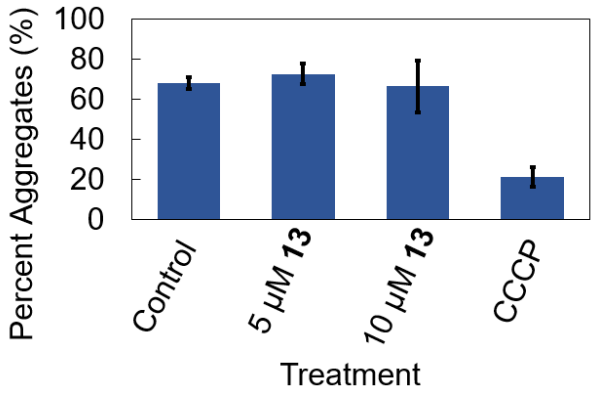

Figure S30. JC-1 assay of **13** for 24 h in HeLa cells. CCCP (300 μM for 15 min) was used as a positive control. Error bars represent one standard deviation.

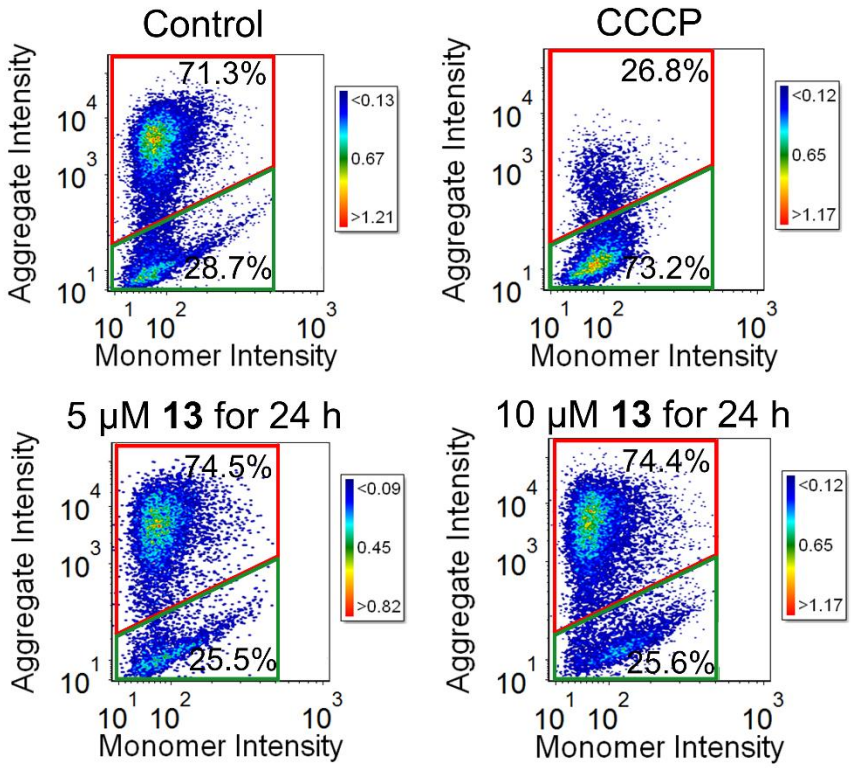

Figure S31. Representative histograms for the analysis of mitochondrial membrane potential by flow cytometry using the JC-1 dye. The red aggregates and green monomers are gated.

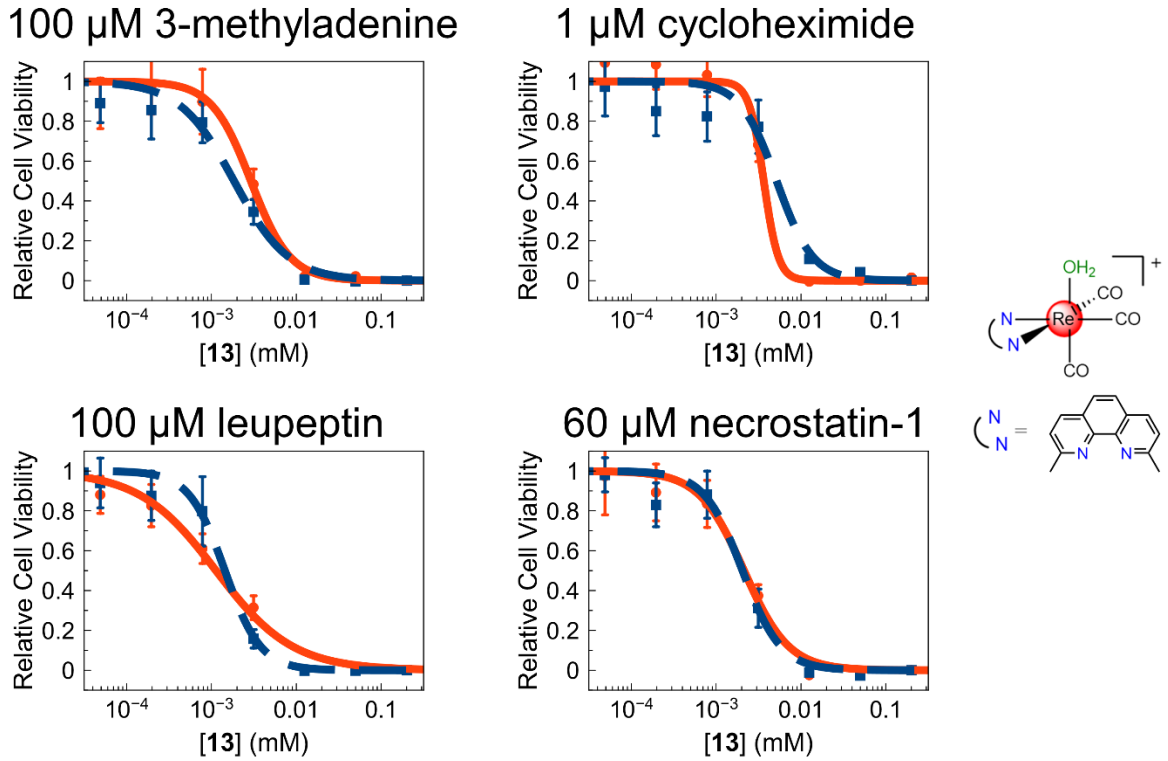

Figure S32. Representative cell viability curves of **13** in HeLa cells in the absence (red circles, solid line) or presence (blue squares, dashed line) of different inhibitors.

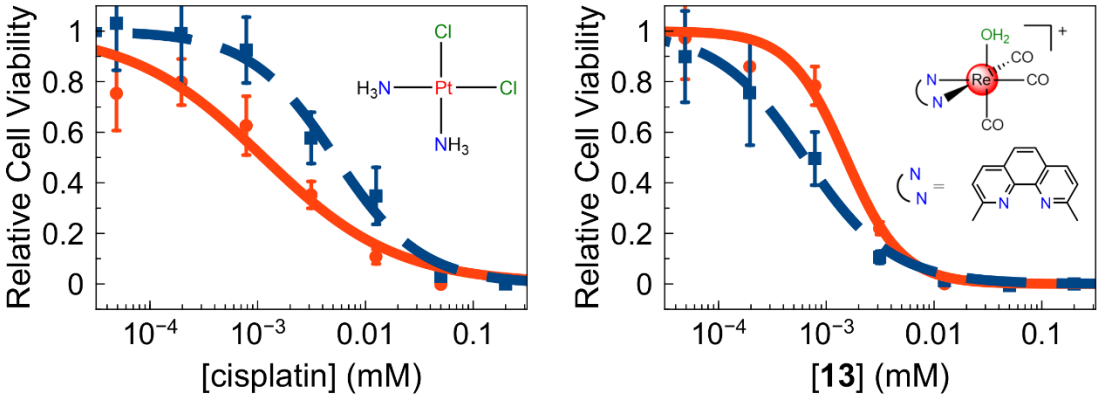

Figure S33. Representative cell viability curves of cisplatin and **13** in HeLa cells without (red circles, solid line) or with (blue squares, dashed line) 15 μM of the pan-caspase inhibitor Z-VAD-FMK.

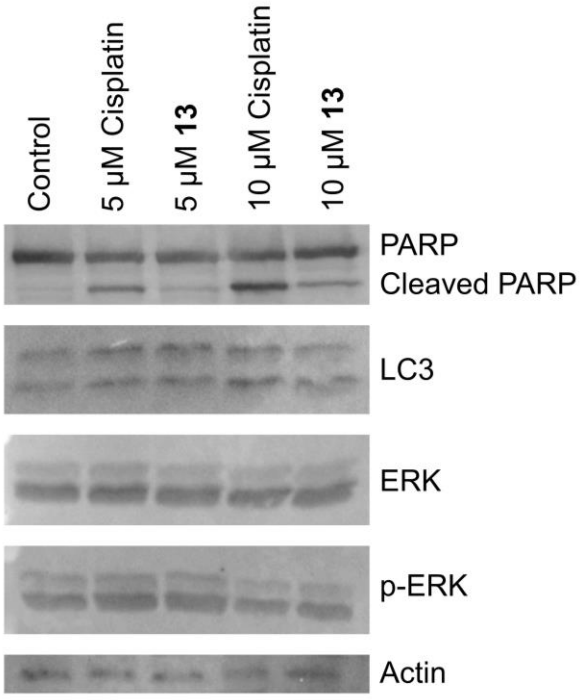

Figure S34. Western blots of HeLa cell lysate from control cells or cells treated with **13** or cisplatin.

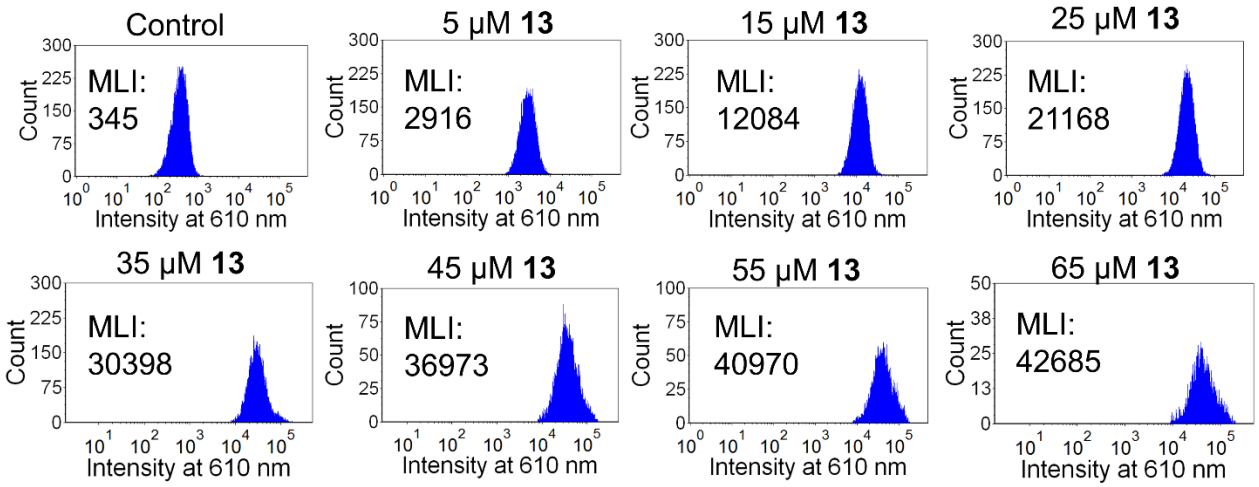

Figure S35. Histograms of the 4 h concentration-dependent uptake analysis of **13** by flow cytometry. MLI = mean luminescence intensity.

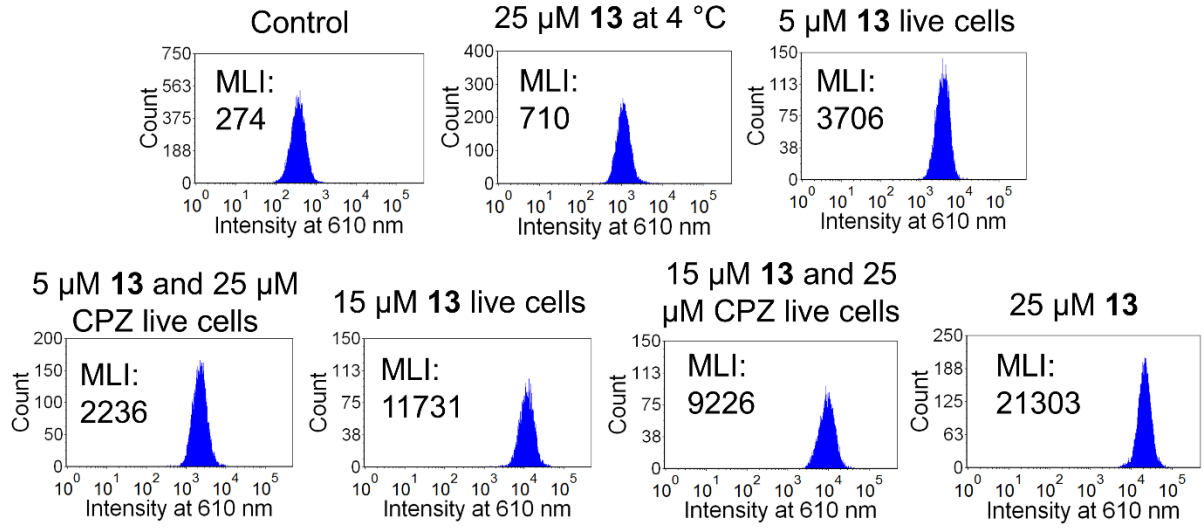

Figure S36. Representative histograms of the 4 h uptake mechanism analysis of **13** by flow cytometry. MLI = mean luminescence intensity, CPZ = chlorpromazine, live cells = propidium iodide negative cells.

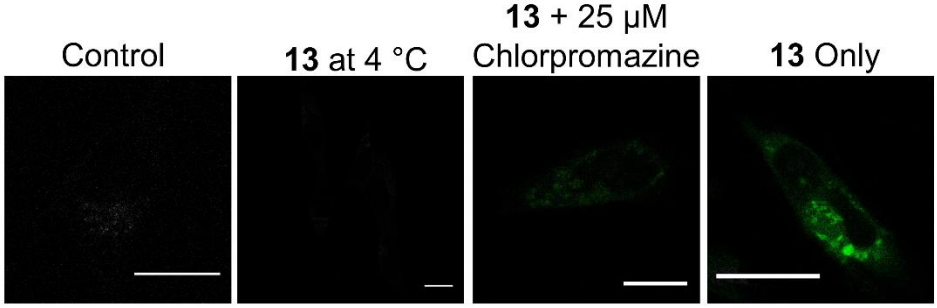

Figure S37. Fluorescence microscope images of HeLa cells to support the flow cytometry data for the uptake of **13**. In the figure, **13** represents 25 μM **13** for 4 h. All images were taken with the same microscope settings. Scale bars = 20 μm.

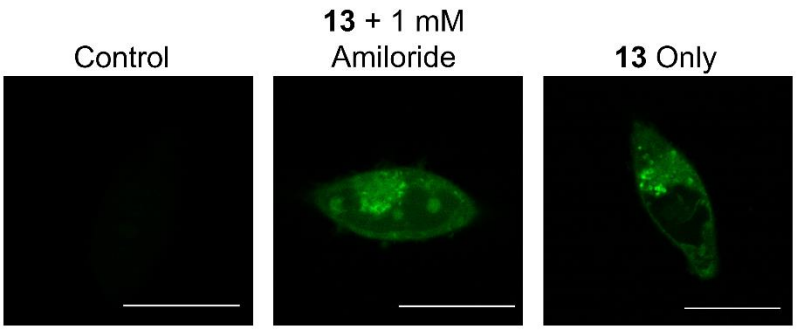

Figure S38. Fluorescence microscope images of HeLa cells in the presence or absence of the micropinocytosis inhibitor amiloride. In the figure, **13** represents 25 µM **13** for 4 h. All images were taken with the same microscope settings. Scale bars = 20 µm.

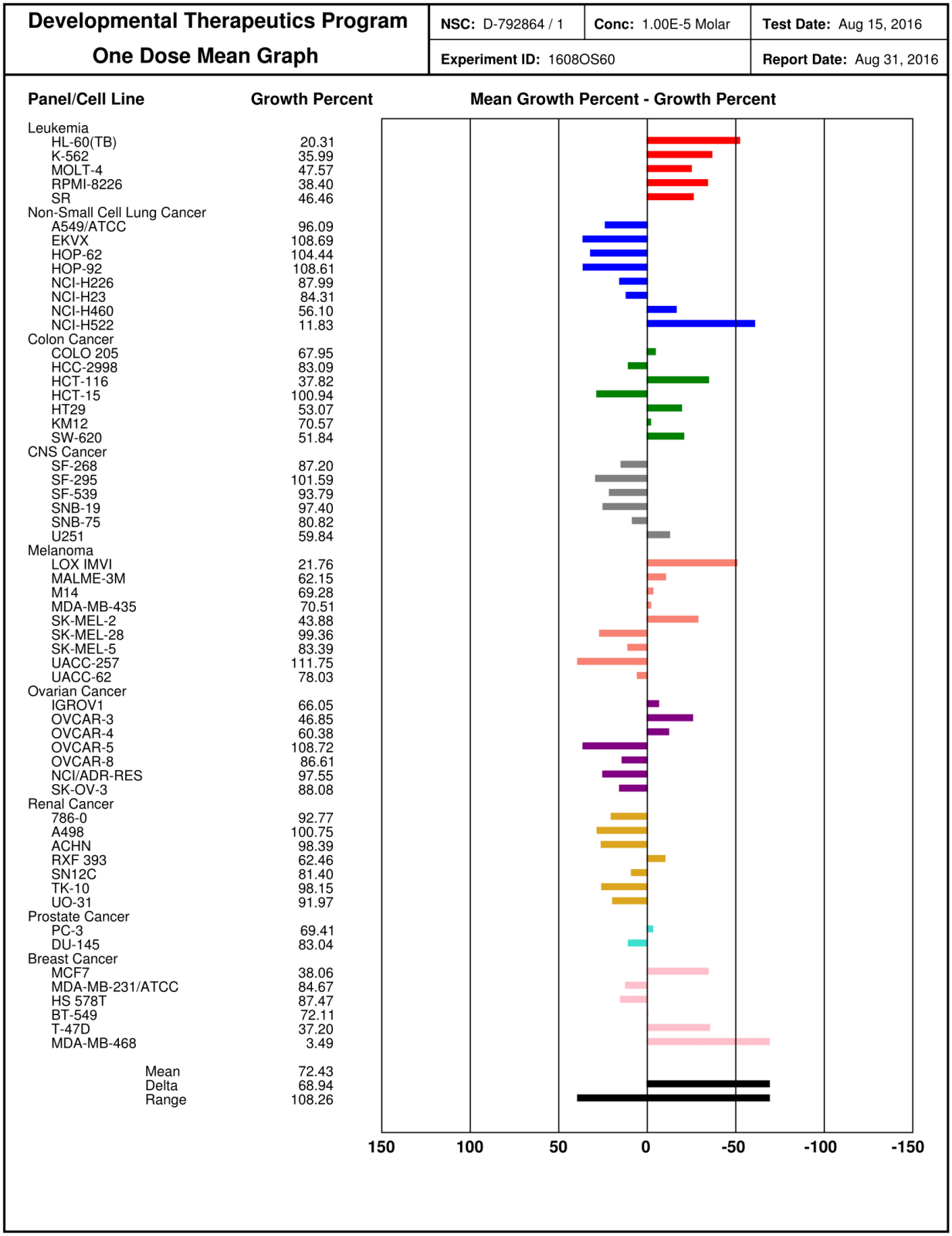

Figure S39. NCI-60 one dose mean graph for 10 μM **13**.

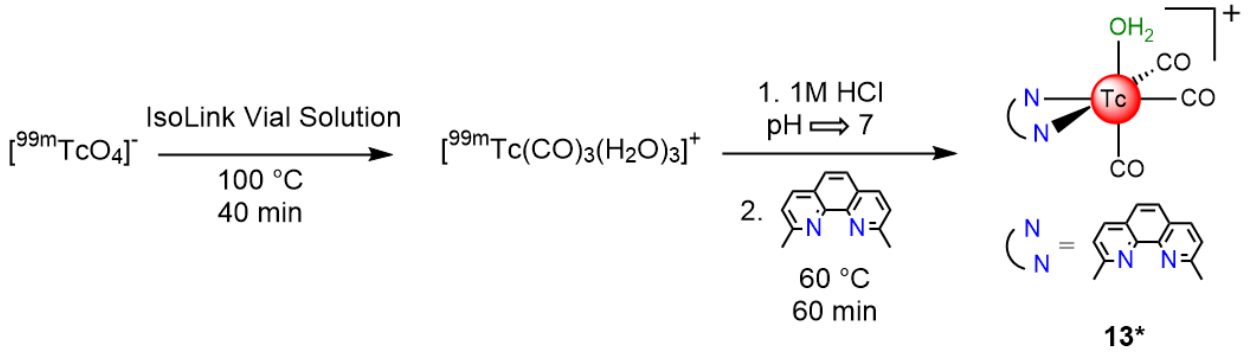

Figure S40. Synthesis of **13***.

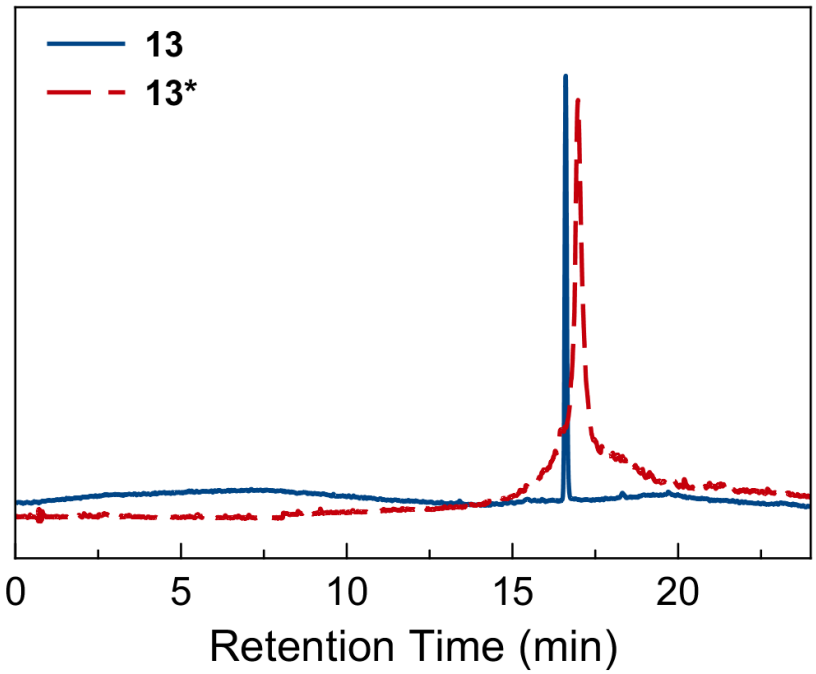

Figure S41. HPLC traces of **13** (monitoring 254 nm) and **13*** (monitoring with a gamma counter).

Table S1. Biodistribution data for the Re (**13**) and ^{99m}Tc tricarbonyl (**13***) complexes with the dmphen ligand. Error represents one standard deviation.

Organ, Tissue, or Fluid	**13** (%ID/g) 30 min (n = 3)	60 min (n = 4)	90 min (n = 4)	**13*** (%ID/g) 30 min (n = 3)	60 min (n = 4)	90 min (n = 4)
Blood	1.38 ± 0.99	0.44 ± 0.15	0.34 ± 0.11	9.37 ± 1.03	5.63 ± 0.92	4.25 ± 0.49
Heart	4.28 ± 2.79	3.15 ± 0.62	2.42 ± 0.24	4.17 ± 1.83	3.24 ± 0.88	2.68 ± 0.85
Liver	23.82 ± 6.58	19.62 ± 4.46	22.93 ± 3.16	49.3 ± 3.88	32.74 ± 4.53	32.44 ± 2.65
Kidney	25.59 ± 10.88	18.92 ± 4.39	14.79 ± 4.34	13.28 ± 3.48	6.27 ± 3.87	4.01 ± 3.12
Ovaries	1.07 ± 1.01	0.72 ± 0.08	0.76 ± 0.44	0.99 ± 0.87	0.51 ± 0.20	0.40 ± 0.26
Bone	1.12 ± 0.61	0.84 ± 0.35	0.50 ± 0.34	0.97 ± 0.80	0.66 ± 0.46	0.51 ± 0.31
Muscle	0.35 ± 0.05	0.45 ± 0.09	0.49 ± 0.1	0.40 ± 0.26	0.11 ± 0.07	0.24 ± 0.14
Urine	13.23[†] ± 0.45	16.65 ± 7.68	12.06[‡] ± 6.62	17.7 ± 1.98	21.0 ± 14.28	13.93 ± 7.51

[†]n=2, [‡]n=3

Table S2. Reagent suppliers.

Reagent	Origin
rhenium pentacarbonyl chloride	Pressure Chemical Co.
cis-diamminedichloroplatinum(II) (cisplatin)	Alfa Aesar
2,2’-bipyridine	Alfa Aesar
4,4’-dimethyl-2,2’-bipyridyl	Sigma-Aldrich
4,4’-dimethoxy-2,2’-bipyridine	Sigma-Aldrich
dimethyl 2,2’-bipyridine-4,4’-dicarboxylate	Sigma-Aldrich
1,10-phenanthroline	Strem Chemicals
2,9-dimethyl-1,10-phenanthroline	Alfa Aesar
4,7-diphenyl-1,10-phenanthroline	Sigma-Aldrich
silver triflate	Strem Chemicals
silver nitrate	Strem Chemicals
silver tetrafluoroborate	Sigma-Aldrich
fetal bovine serum	Gibco
DMEM, RPMI, MEM	Corning
100 mM sodium pyruvate	Corning
3-(4,5-dimethylthiazol-2-yl)-2,5-diphenyltetrazolium bromide (MTT)	Chem-Impex
all deuterated solvents	Cambridge Isotope Laboratories
propidium iodide	Alfa Aesar
ribonuclease A	Amresco
2’,7’-dichlorofluorescin diacetate	Sigma-Aldrich
annexin-V Alexa Fluor 488	Thermo Fisher Scientific, A13201
annexin binding buffer	Thermo Fisher Scientific
JC-1	Cayman Chemical
carbonyl cyanide m-chlorophenylhydrazone (CCCP)	Sigma-Aldrich
Z-VAD-FMK	Cayman Chemical
Lipofectamine® 2000	Thermo Fisher Scientific
Transfectagro™	Corning
LysoTracker® Red DND-99	Thermo Fisher Scientific
Hoechst 33342	Thermo Fisher Scientific
bovine serum albumin	Amresco
etoposide	AdipoGen
3-methyladenine	Acros Organics
cycloheximide	Amresco
leupeptin	Cayman Chemical
necrostatin-1	Cayman Chemical
2-aminoethoxydiphenyl borate	Sigma-Aldrich
chlorpromazine•HCl	TCI
N-acetyl L-histidine monohydrate	TCI
9-ethylguanine, *N*-acetyl L-cysteine	Sigma-Aldrich
L-serine, L-methionine	Sigma-Aldrich
L-glycine	Eastman Chemical

Table S3. Crystal data and structure refinement for **9**-NO_3.

Empirical formula	$ReC_{18}H_{18}N_3O_7$	
Formula weight	574.55	
Temperature	223(2) K	
Wavelength	0.71073 Å	
Crystal system	Monoclinic	
Space group	$P2_1/n$	
Unit cell dimensions	a = 7.3208(6) Å	α= 90°
	b = 18.2693(18) Å	β= 99.887(5)°
	c = 15.3665(13) Å	γ = 90°
Volume	2024.7(3) $Å^3$	
Z	4	
Density (calculated)	1.885 Mg/m^3	
Absorption coefficient	6.046 mm^{-1}	
F(000)	1112	
Crystal size	0.150 x 0.090 x 0.060 mm^3	
Theta range for data collection	1.747 to 27.348°.	
Index ranges	-8<=h<=8, -22<=k<=22, -18<=l<=18	
Reflections collected	17464	
Independent reflections	3698 [R(int) = 0.0440]	
Completeness to theta = 25.242°	100.0 %	
Absorption correction	Semi-empirical from equivalents	
Max. and min. transmission	0.7461 and 0.6374	
Refinement method	Full-matrix least-squares on F^2	
Data / restraints / parameters	3698 / 0 / 266	
Goodness-of-fit (GoF)[c] on F^2	1.094	
Final R indices [I>2sigma(I)]	R1[a] = 0.0305, wR2[b] = 0.0688	
R indices (all data)	R1[a] = 0.0380, wR2[b] = 0.0722	
Extinction coefficient	n/a	
Largest diff. peak and hole	2.010 and -0.520 e.$Å^{-3}$	

[a] $R1 = \Sigma||Fo| - |Fc||/\Sigma|Fo|$ for all data. [b] $wR2 = \{\Sigma[w(Fo^2 - Fc^2)^2]/\Sigma[w(Fo^2)^2]\}^{1/2}$. [c] $GoF = \{\Sigma[w(Fo^2 - Fc^2)^2]/(n - p)\}^{1/2}$, where n is the number of data and p is the number of refined parameters.

Table S4. Crystal data and structure refinement for **10**-BF_4.

Empirical formula	$ReC_{17}H_{15}N_3O_5B_{0.93}F_{3.73}Cl_{0.07}$	
Formula weight	610.81	
Temperature	223.15 K	
Wavelength	0.71073 Å	
Crystal system	Monoclinic	
Space group	$P2_1/n$	
Unit cell dimensions	a = 9.9967(7) Å	α= 90°
	b = 17.2578(12) Å	β= 97.033(3)°
	c = 12.1669(9) Å	γ = 90°
Volume	2083.3(3) $Å^3$	
Z	4	
Density (calculated)	1.947 Mg/m^3	
Absorption coefficient	5.908 mm^{-1}	
F(000)	1169	
Crystal size	0.3 x 0.15 x 0.13 mm^3	
Theta range for data collection	2.368 to 28.699°.	
Index ranges	-7<=h<=13, -23<=k<=23, -16<=l<=16	
Reflections collected	22625	
Independent reflections	5369 [R(int) = 0.0267]	
Completeness to theta = 25.242°	99.5 %	
Absorption correction	Semi-empirical from equivalents	
Max. and min. transmission	0.7461 and 0.5849	
Refinement method	Full-matrix least-squares on F^2	
Data / restraints / parameters	5369 / 0 / 284	
Goodness-of-fit (GoF)[c] on F^2	1.034	
Final R indices [I>2sigma(I)]	R1[a] = 0.0202, wR2[b] = 0.0426	
R indices (all data)	R1[a] = 0.0259, wR2[b] = 0.0444	
Extinction coefficient	n/a	
Largest diff. peak and hole	0.843 and -0.589 e.$Å^{-3}$	

[a] $R1 = \Sigma||F_o| - |F_c||/\Sigma|F_o|$ for all data. [b] $wR2 = \{\Sigma[w(F_o^2 - F_c^2)^2]/\Sigma[w(F_o^2)^2]\}^{1/2}$. [c] $GoF = \{\Sigma[w(F_o^2 - F_c^2)^2]/(n - p)\}^{1/2}$, where n is the number of data and p is the number of refined parameters.

Table S5. Crystal data and structure refinement for **11**.

Empirical formula	$ReC_{18}H_{12}N_2O_{10}SF_3$	
Formula weight	691.56	
Temperature	223(2) K	
Wavelength	0.71073 Å	
Crystal system	Triclinic	
Space group	$P\bar{1}$	
Unit cell dimensions	a = 9.3515(8) Å	α= 74.264(4)°
	b = 9.5031(8) Å	β= 89.405(4)°
	c = 13.1788(11) Å	γ = 85.789(4)°
Volume	1124.18(17) $Å^3$	
Z	2	
Density (calculated)	2.043 Mg/m^3	
Absorption coefficient	5.580 mm^{-1}	
F(000)	664	
Crystal size	0.170 x 0.140 x 0.070 mm^3	
Theta range for data collection	2.184 to 25.347°.	
Index ranges	-11<=h<=11, -11<=k<=10, -15<=l<=15	
Reflections collected	19763	
Independent reflections	4127 [R(int) = 0.0306]	
Completeness to theta = 25.242°	100.0 %	
Absorption correction	Semi-empirical from equivalents	
Max. and min. transmission	0.7461 and 0.5873	
Refinement method	Full-matrix least-squares on F^2	
Data / restraints / parameters	4127 / 0 / 318	
Goodness-of-fit (GoF)[c] on F^2	1.097	
Final R indices [I>2sigma(I)]	R1[a] = 0.0198, wR2[b] = 0.0436	
R indices (all data)	R1[a] = 0.0216, wR2[b] = 0.0443	
Extinction coefficient	n/a	
Largest diff. peak and hole	1.375 and -0.496 e.$Å^{-3}$	

[a] $R1 = \Sigma||Fo| - |Fc||/\Sigma|Fo|$ for all data. [b] $wR2 = \{\Sigma[w(Fo^2 - Fc^2)^2]/\Sigma[w(Fo^2)^2]\}^{1/2}$. [c] $GoF = \{\Sigma[w(Fo^2 - Fc^2)^2]/(n - p)\}^{1/2}$, where n is the number of data and p is the number of refined parameters.

Table S6. Crystal data and structure refinement for **13**.

Empirical formula	$ReC_{18}H_{14}N_2O_7SF_3$	
Formula weight	645.57	
Temperature	223(2) K	
Wavelength	0.71073 Å	
Crystal system	Triclinic	
Space group	$P\bar{1}$	
Unit cell dimensions	a = 8.7357(5) Å	α= 64.877(3)°
	b = 11.4690(7) Å	β= 88.601(2)°
	c = 12.1592(7) Å	γ= 75.881(2)°
Volume	1065.31(11) $Å^3$	
Z	2	
Density (calculated)	2.013 Mg/m^3	
Absorption coefficient	5.870 mm^{-1}	
F(000)	620	
Crystal size	0.330 x 0.120 x 0.100 mm^3	
Theta range for data collection	1.857 to 30.034°.	
Index ranges	-12<=h<=12, -16<=k<=16, -17<=l<=17	
Reflections collected	23532	
Independent reflections	6226 [R(int) = 0.0247]	
Completeness to theta = 25.242°	99.9 %	
Absorption correction	Semi-empirical from equivalents	
Max. and min. transmission	0.7461 and 0.6089	
Refinement method	Full-matrix least-squares on F^2	
Data / restraints / parameters	6226 / 2 / 297	
Goodness-of-fit (GoF)[c] on F^2	1.064	
Final R indices [I>2sigma(I)]	R1[a] = 0.0261, wR2[b] = 0.0622	
R indices (all data)	R1[a] = 0.0308, wR2[b] = 0.0642	
Extinction coefficient	n/a	
Largest diff. peak and hole	2.132 and -0.568 e.$Å^{-3}$	

[a] $R1 = \Sigma||Fo| - |Fc||/\Sigma|Fo|$ for all data. [b] $wR2 = \{\Sigma[w(Fo^2 - Fc^2)^2]/\Sigma[w(Fo^2)^2]\}^{1/2}$. [c] $GoF = \{\Sigma[w(Fo^2 - Fc^2)^2]/(n - p)\}^{1/2}$, where n is the number of data and p is the number of refined parameters.

References

(1) Smieja, J. M.; Kubiak, C. P. *Inorg. Chem.* **2010**, *49*, 9283–9289.
(2) Kurz, P.; Probst, B.; Spingler, B.; Alberto, R. *Eur. J. Inorg. Chem.* **2006**, *2006*, 2966–2974.
(3) Sheldrick, G. M. *Acta Crystallogr., Sect. C: Struct. Chem.* **2015**, *71*, 3–8.
(4) Sheldrick, G. M. *Acta Crystallogr., Sect. A: Found. Crystallogr.* **2007**, *64*, 112–122.
(5) Shen, D. W.; Akiyama, S.; Schoenlein, P.; Pastan, I.; Gottesman, M. M. *Br. J. Cancer* **1995**, *71*, 676–683.
(6) Akiyama, S.; Fojo, A.; Hanover, J. A.; Pastan, I.; Gottesman, M. M. *Somat. Cell Mol. Genet.* **1985**, *11*, 117–126.
(7) Godwin, A. K.; Meister, A.; O'Dwyer, P. J.; Huang, C. S.; Hamilton, T. C.; Anderson, M. E. *Proc. Natl. Acad. Sci. U. S. A.* **1992**, *89*, 3070–3074.
(8) Barr, M. P.; Gray, S. G.; Hoffmann, A. C.; Hilger, R. A.; Thomale, J.; O'Flaherty, J. D.; Fennell, D. A.; Richard, D.; O'Leary, J. J.; O'Byrne, K. J. *PLoS One* **2013**, *8*, 1–19.
(9) Fallahi-Sichani, M.; Honarnejad, S.; Heiser, L. M.; Gray, J. W.; Sorger, P. K. *Nat. Chem. Biol.* **2013**, *9*, 708–714.
(10) Rieger, A. M.; Nelson, K. L.; Konowalchuk, J. D.; Barreda, D. R. *J. Vis. Exp.* **2011**, e2597.